THE JOURNAL OF BIOLOGICAL CHEMISTRY VOL. 287, NO. 45, pp. 37808–37823, November 2, 2012

Intracellular and Extracellular ATP Coordinately Regulate the Inverse Correlation between Osteoclast Survival and Bone Resorption*[S]

Received for publication, May 25, 2012, and in revised form, September 9, 2012 Published, JBC Papers in Press, September 17, 2012, DOI 10.1074/jbc.M112.385369

Tsuyoshi Miyazaki[‡§1], Mitsuyasu Iwasawa[¶], Tomoki Nakashima[‖], Shuuichi Mori[‡], Kazuhiro Shigemoto[‡], Hiroaki Nakamura[**], Hideki Katagiri[‡‡], Hiroshi Takayanagi[‖], and Sakae Tanaka[¶]

From the [‡]Department of Geriatric Medicine and [§]Department of Orthopaedic Surgery, Tokyo Metropolitan Geriatric Hospital and Institute of Gerontology, 35-2 Sakae-cho, Itabashi-ku, Tokyo 173-0015, the [¶]Department of Orthopaedic Surgery, Faculty of Medicine, University of Tokyo, Hongo 7-3-1, Bunkyo-ku, Tokyo 113-0033, the [‖]Department of Cell Signaling, Graduate School, Tokyo Medical and Dental University, Yushima 1-5-45, Bunkyo-ku, Tokyo 113-8549, the [**]Department of Histology and Cell Biology, Matsumoto Dental University, 1780 Gobara-Hirooka, Shiojiri, Nagano 399-0781, and the [‡‡]Department of Metabolic Diseases, Center for Metabolic Diseases, Tohoku University Graduate School of Medicine, 2-1 Seiryo-machi, Aoba-ku, Sendai 980-8575, Japan

Background: Mature osteoclasts with a spontaneous tendency toward apoptosis resorb bone efficiently during their short lifespan.
Results: Released ATP from intracellular stores has a negative impact on the bone resorption activity of osteoclasts by altering their cytoskeletal structures.
Conclusion: ATP depletion leads to osteoclastic bone resorption.
Significance: This study provides a new direction for investigating the mechanisms involved in physiological and pathological bone resorption.

Osteoclasts, highly differentiated bone-resorbing cells of hematopoietic origin, have two conflicting tendencies: a lower capacity to survive and a higher capacity to execute energy-consuming activities such as bone resorption. Here, we report that when compared with their precursors, mature mitochondria-rich osteoclasts have lower levels of intracellular ATP, which is associated with receptor activator of nuclear factor κ-B ligand (RANKL)-induced Bcl-x_L down-regulation. Severe ATP depletion, caused by disrupting mitochondrial transcription factor A (*Tfam*) gene, leads to increased bone-resorbing activity despite accelerated apoptosis. Although AMP-activated protein kinase (AMPK) activation by ATP depletion is not involved in the regulation of osteoclast function, the release of ATP from intracellular stores negatively regulates bone-resorbing activity through an autocrine/paracrine feedback loop by altering cytoskeletal structures. Furthermore, osteoclasts derived from aged mice exhibit reduced mitochondrial DNA (mtDNA) and intracellular ATP levels with increased bone-resorbing activity, implicating the possible involvement of age-related mitochondrial dysfunction in osteoporosis. Thus, our study provides evidence for a mechanism underlying the control of cellular functions by reciprocal changes in intracellular and extracellular ATP, which regulate the negative correlation between osteoclast survival and bone resorption.

Osteoclasts are large, multinucleated, motile cells that are formed by fusion of hematopoietic cells of monocyte/macrophage lineage (1, 2). They are unique cells in the body that are able to degrade the extracellular bone matrix. The lifespan of mature osteoclasts is relatively short both *in vitro* and *in vivo*. Once differentiated, they rapidly die in the absence of supporting cells such as osteoblasts, bone marrow stromal cells, or growth factors such as M-CSF, RANKL,[2] and IL-1 (3). Despite their short lifespan, osteoclasts execute their duties by special attachment to the bone, synthesis and secretion of hydrochloric acid and powerful proteases, internalization of extracellular bone matrix degradation products, and efficient migration along the bone surface. However, the mechanism by which apoptosis-sensitive osteoclasts complete these energy-consuming activities is poorly understood. Recently, the roles of Bcl-2 family members, including proapoptotic Bim and antiapoptotic Bcl-x_L, in osteoclast apoptosis have been well studied, revealing the interesting relationship between osteoclast survival and bone resorption. $Bim^{-/-}$ osteoclasts showed decreased bone-resorbing activity despite prolonged survival (4), whereas *Bcl-x*-deficient osteoclasts exhibited increased bone resorption with accelerated apoptosis (5), implicating the existence of an as yet unidentified mechanism in the regulation of this inverse correlation.

* This work was in part supported by grants-in-aid for scientific research from the Japan Society for the Promotion of Science.
[S] This article contains supplemental Figs. S1–S3.
[1] To whom correspondence should be addressed: Dept. of Geriatric Medicine, Tokyo Metropolitan Geriatric Hospital and Institute of Gerontology, 35-2 Sakae-cho, Itabashi-ku, Tokyo 173-0015, Japan. Tel.: 81-3-3964-3241 (ext. 3012); Fax: 81-3-3579-4776; E-mail: miyazak14@tmig.or.jp.

[2] The abbreviations used are: RANKL, receptor activator of nuclear factor κ-B ligand; AMPK, AMP-activated protein kinase; cKO, conditional knockout; Pyk2, proline-rich tyrosine kinase; Tfam, mitochondrial transcription factor A; α-MEM, α-minimum Eagle's medium; ATPγS, adenosine 5′-*O*-(3-thiotriphosphate); TRAP, tartrate-resistant acid phosphatase; BMM, bone marrow-derived monocyte/macrophage precursor cell; NFATc1, nuclear factor of activated T cells c1; Csk, C-Src tyrosine kinase; BzATP, 2′,3′-*O*-(4-benzoylbenzoyl)-ATP; Oc.N., osteoclast number; ES, eroded surface; BS, bone surface; DN, dominant negative; CA, constitutively active.

ATP is a ubiquitous carrier of chemical energy and a building block of genetic material in all living organisms. ATP also serves as an extracellular signaling molecule involved in vascular tone, synaptic transmission, and cell death (6, 7). Cellular ATP levels have been reported to reflect cell viability, including cell survival, cell growth, and morphology (8, 9). Furthermore, it has been reported that complete ATP depletion (<5% of control) results in necrosis, and partial ATP depletion (~10–65% of control) induces apoptosis, as evidenced by internucleosomal DNA cleavage, changes in cellular morphology, and alterations in the plasma membrane (10). Most of the ATP supply of the cell is produced in the mitochondria, and its biogenesis depends on the coordinated expression of genes in the nucleus and mitochondria.

Mitochondria have their own genomic system: namely, mitochondrial DNA (mtDNA), which is a closed-circular double-stranded DNA. mtDNA encodes 13 key subunits of the respiratory chain; therefore, mtDNA expression is critical for mitochondrial biogenesis and normal cellular function (11). mtDNA copy number is decreased not only in mtDNA mutation diseases, but also in a wide variety of acquired degenerative and ischemic diseases (12). To study the role of intracellular ATP in osteoclast function, we employed the *cre-loxP* recombination system to disrupt the nuclear gene for mitochondrial transcription factor A (*Tfam*). Tfam is necessary for mtDNA maintenance in mammals and regulates mtDNA copy number by directly binding and coating mtDNA (13, 14). In addition, Tfam is absolutely required for transcription initiation at mtDNA promoters (15). In fact, disruption of the *Tfam* gene causes depletion of mtDNA, loss of mitochondrial transcripts, loss of mtDNA-encoded polypeptides, severe respiratory chain deficiency, and reduced ATP production (8, 13, 16, 17).

In this study, we characterized mitochondria-rich osteoclasts as ATP-depleted cells and identified Bcl-x_L as a regulator of intracellular ATP levels in mature osteoclasts. Furthermore, we demonstrated that ATP depletion following *Tfam* deficiency leads to increased bone-resorbing activity despite accelerated apoptosis, and the release of endogenous ATP negatively regulates osteoclast function through an autocrine/paracrine feedback loop. Osteoclasts derived from aged mice exhibited reduction of mtDNA copy number and intracellular ATP with increased bone-resorbing activity. These findings highlight a previously unknown mechanism by which intracellular ATP levels regulate the inverse correlation between osteoclast survival and bone resorption.

EXPERIMENTAL PROCEDURES

Animals—*Tfam*$^{flox/flox}$ mice of C57BL/6 background (13) were mated to cathepsin K-Cre mice, in which the Cre recombinase gene is knocked into the cathepsin K locus and is specifically expressed in osteoclasts (18). Cathepsin K-Cre$^{+/-}$ *Tfam*$^{flox/flox}$ (cKO) and cathepsin K-Cre$^{-/-}$ *Tfam*$^{flox/flox}$ (normal littermates) mice were generated by mating cathepsin K-Cre$^{-/-}$ *Tfam*$^{flox/flox}$ male mice with cathepsin K-Cre$^{+/-}$ *Tfam*$^{flox/+}$ female mice. *P2rx7*$^{-/-}$ mice, generated as described previously (19), were obtained from The Jackson Laboratory. All animals were housed under specific pathogen-free conditions and treated with humane care under approval from the Animal Care and Use Committee of the Tokyo Metropolitan Institute of Gerontology.

Analysis of Bone Phenotype—Radiography was performed using a high-resolution soft x-ray system (Softex). Micro-computed tomography scanning was performed using a ScanXmate-A100S Scanner (Comscan Techno). Three-dimensional microstructural image data were reconstructed, and structural indices were calculated using the TRI/3D-BON software (RATOC). Bone histomorphometric analyses were performed as described (5). TRAP-positive cells were stained at pH 5.0 in the presence of L(+)-tartaric acid using naphthol AS-MX phosphate (Sigma-Aldrich) in *N*,*N*-dimethyl formamide (Wako Pure Chemical) as the substrate.

Generation of Osteoclasts and Survival/Bone Resorption Assay—Bone marrow cells were obtained from the femur and tibia of male mice, and bone marrow macrophages were cultured in α-MEM (Invitrogen) containing 10% FBS (Sigma-Aldrich) in the presence of 100 ng/ml M-CSF (R&D Systems) for 2 days. Osteoclasts were generated by stimulating bone marrow macrophages with 10 ng/ml M-CSF and 100 ng/ml RANKL (Wako Pure Chemical) for an additional 4–5 days or by the coculture system established by Takahashi *et al.* (20). The survival assay was performed as follows (5). After osteoclasts were generated, both RANKL and M-CSF were removed from the culture (time 0), and osteoclasts were cultured for the indicated times. The survival rate of the cells was estimated as the percentage of morphologically intact TRAP-positive multinucleated cells when compared with those at time 0. The bone resorption assay was performed as described previously (21). Briefly, osteoclasts were generated by coculturing osteoblasts and bone marrow cells on collagen gel-coated dishes in the presence of 10 nM 1α,25(OH)$_2$vitamin D_3 and 1 μM prostaglandin E_2. On day 6 of culture, when osteoclasts were differentiated, the cells were dispersed by treating with 0.1% bacterial collagenase (Wako Pure Chemical) for 10 min. The cells were resuspended in α-MEM containing 10% FBS, replated on dentine slices, and cultured for 12 h. After cells were removed by treating the dentine slices with 1 M NH_4OH, the resorption areas were visualized by staining with 1% toluidine blue. The resorption pit area was quantified using an image analysis system (Microanalyzer, Nihon Poladigital).

Retroviral Gene Transfer—For production of retrovirus, full-length cDNA of mouse *Bcl-x_L* was inserted into pMx vectors. For gene silencing, an RNAi sequence was designed for the mouse *Bcl-x_L* gene. The targeting sequence used was GCGTTCAGTGATCTAACATCC (22). The RNAi expression vector for this gene was constructed with piGENEmU6 vector (for mouse; iGENE Therapeutics). For retrovirus expressing RNAi, the U6 promotor and inserts in piGENE vectors were cloned into pMx vectors. Bone marrow-derived monocyte/macrophage precursor cells (BMMs) (5×10^6 cells) were incubated with 8 ml of retrovirus stock for 6 h in the presence of Polybrene (6 μg/ml) and recombinant mouse M-CSF (30 ng/ml). After 6 h of retrovirus infection, the medium was changed to α-MEM containing 10% FBS and M-CSF (100 ng/ml) for 48 h. After the BMMs were lifted with trypsin, the cells were selected by incubating with α-MEM, 10% FBS con-

taining 2 mg/ml puromycin for 2 days. Puromycin-resistant cells were used for further experiments.

Adenoviral Gene Transfer—Adenoviral infection of osteoclasts was performed as reported previously (23). In short, on day 5, when osteoclasts began to appear, mouse cocultures were incubated for 1 h at 37 °C with a small amount of α-MEM containing recombinant adenoviruses at a multiplicity of infection of 100. Cells were then washed twice with PBS and further incubated with α-MEM containing 10% FBS, 10 nM $1\alpha,25(OH)_2D_3$, and 1 μM prostaglandin E_2 at 37 °C. Experiments were performed 2–3 days after infection.

Western Blotting, Triton X-insoluble Cytoskeleton, and Immunofluorescence Staining—BMMs and osteoclasts were harvested, and cell lysates were subjected to immunoblot analysis with specific antibodies against Tfam (Aviva Systems Biology), Cre (Covance), nuclear factor of activated T cells c1 (NFATc1) (Santa Cruz Technology), v-Src (Sigma), fodrin (Millipore), proline-rich tyrosine kinase 2 (Pyk2), Bcl-x_L, Bim, cleaved caspase-3, β-actin, phospho-AMPK, AMP-activated protein kinase (AMPK), and phospho-tyrosine (Cell Signaling Technology). To isolate Triton X-insoluble cytoskeletons, cells were washed once with isotonic buffer (20 mM Hepes, pH 7.5, 150 mM NaCl, 0.5 mM EDTA, 1 mM DTT, 4 mM $MgCl_2$, 1 mM PMSF, 15 μg/ml aprotinin), treated with 0.05% Triton X-100/isotonic (+) buffer (isotonic buffer supplemented with 0.5 mM ATP, 2% BSA) for 1 min, and washed twice with isotonic (+) buffer (24, 25). For immunofluorescence staining, cells were fixed in 4% paraformaldehyde, permeabilized, and treated with the indicated specific antibodies followed by staining with Alexa Fluor 488- or 546-labeled secondary antibody (Molecular Probes). Confocal images were acquired with a Leica confocal laser-scanning unit, TCS SP5, using a 63× glycerin objective on a Leica DMI6000 microscope (Leica Microsystems).

Mitochondrial Fractionation—Mitochondria-enriched fractions were isolated using a mitochondria isolation kit for cultured cells (Thermo Scientific) according to the manufacturer's instructions. The pelleted mitochondria of BMMs, osteoclasts, and osteoblasts were lysed in the lysis buffer provided in the presence of protease inhibitors. The protein content of the mitochondrial fractions was expressed as the percentage of total protein of the corresponding whole-cell extract. Protein concentration was determined using the Bradford method.

ATP Assay—Prior to measurement of ATP release, culture medium was removed, cell layers were washed, and cells were incubated with serum-free α-MEM. Samples were collected after 1 h and immediately snap-frozen on dry ice for later ATP quantification (26). Intracellular ATP levels and ATP release were assayed using ATPlite (PerkinElmer Life Sciences) according to the manufacturer's instructions. Luminescence was measured using an EnVision multilabel reader (PerkinElmer Life Sciences). The standard curve for ATP was made with a series of dilutions. ATP concentrations were normalized for protein concentration determined by the Bradford method.

Electron Microscopy—Mice were transcardially perfused with 2% paraformaldehyde and 2.5% glutaraldehyde in phosphate buffer (pH 7.4). Femurs and tibiae were immersed in the same fixative for 24 h and demineralized with 10% EDTA (pH 7.4) for 1 week at 4 °C. After post-fixation with 2% OsO_4 in 0.1 M phosphate buffer (pH 7.4) for 1 h at 4 °C, specimens were dehydrated in graded acetone and embedded in Epon 812 (TAAB Laboratories Equipment Ltd.). Ultrathin sections were cut using an ultramicrotome (Ultracut UCT; Leica Microsystems K.K.) and stained with uranyl acetate and lead citrate. These sections were observed under a transmission electron microscope (H-7600; Hitachi High Technologies Co.) at an accelerating voltage of 80 kV.

Real-time PCR—Total RNA was extracted with RNeasy (Qiagen), and an aliquot (1 μg) was reverse-transcribed using a QuantiTect reverse transcription kit (Qiagen) to make single-stranded cDNA. PCR was performed on a 7300 Real-Time PCR system (Applied Biosystems) using QuantiTect SYBR Green PCR master mix (Qiagen) according to the manufacturer's instructions. All reactions were run in triplicate. After data collection, the mRNA copy number of a specific gene in total RNA was calculated with a standard curve generated with serially diluted plasmids containing PCR amplicon sequences and normalized to total RNA with β-actin as an internal control. Primers for endogenous Bcl-x_L were 5′-GCTGGGACACTTTTGTGGAT-3′ and 5′-TGTCTGGTCACTTCCGACTG-3′; primers for β-actin were 5′-AGATGTGGATCAGCAAGCAG-3′ and 5′-GCGCAAGTTAGGTTTTGTCA-3′; primers for Tfam were 5′-CAAAGGATGATTCGGCTCAG-3′ and 5′-AAGCTGAATATATGCCTGCTTTTC-3′; and primers for P2rx7 were 5′-CTCCAAGCTCTTCCATAAGCTC-3′ and 5′-CAGCAAGGGATCCTGGTAAA-3′.

mtDNA Quantitation—mtDNA copy number per nuclear genome in osteoclasts was quantitated as described previously (27). Total DNA purification was performed using the DNeasy kit (Qiagen). The abundance of nuclear and mitochondrial DNA was quantified by real-time PCR under standard conditions using a QuantiTect SYBR Green PCR kit (Qiagen). The primers used for mtDNA were CCTATCACCCTTGCCATCAT and GAGGCTGTTGCTTGTGTGAC. For nuclear DNA (platelet endothelial cell adhesion molecule (PECAM)), ATGGAAAGCCTGCCATCATG and TCCTTGTTGTTCAGCATCAC were used. The ratios between mtDNA and nuclear DNA concentrations were graphed.

Statistics—Statistical analyses were performed using a two-tailed unpaired Student's *t* test or analysis of variance analysis, and each series of experiments was repeated at least three times. Results are presented as mean ± S.D.

RESULTS

Mature Mitochondria-rich Osteoclasts Exhibit Lower Intracellular ATP Levels—Mitochondria are responsible for metabolism or the conversion of energy and oxygen into molecules that enable cells to carry out their various functions. More mitochondria means that a cell has a higher capacity to do work. Although mature osteoclasts are characterized as mitochondria-rich cells, the precise roles of mitochondria in osteoclasts have remained largely elusive. The quantification of isolated mitochondria-enriched fractions showed that mitochondrial protein content in mature osteoclasts was higher than that in BMMs or osteoblasts (Fig. 1*A*). Unexpectedly, intracellular ATP levels in osteoclasts were markedly lower than those in both osteoblasts and BMMs (Fig. 1*B*). These find-

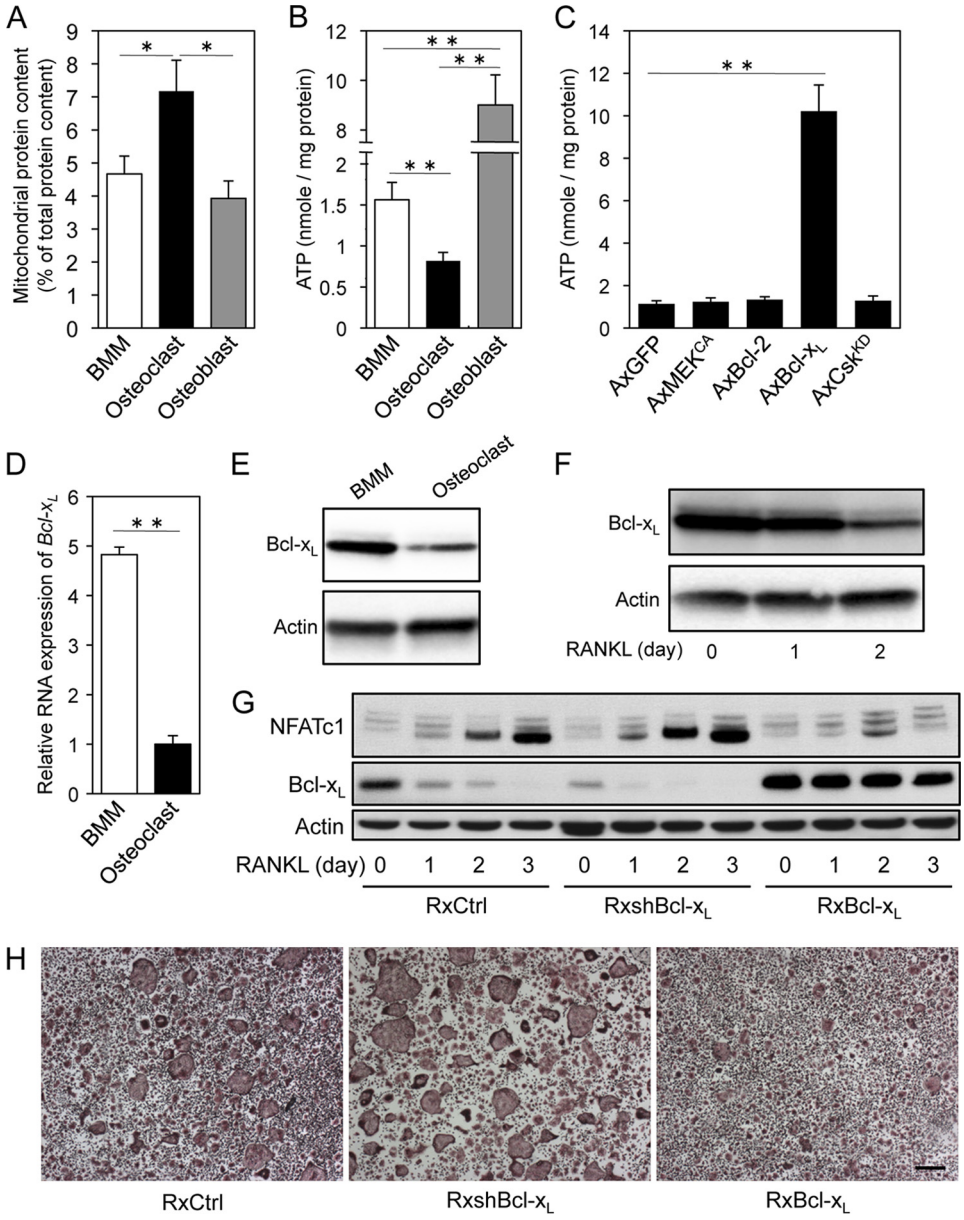

FIGURE 1. **Mature osteoclasts display lower intracellular ATP levels associated with decreased expression of Bcl-x_L.** *A*, mitochondrial protein content in BMMs, osteoclasts, and osteoblasts. The protein content of the mitochondrial fractions was expressed as the percentage of total protein of the corresponding whole-cell extract. Mitochondrial protein content in mature osteoclasts was higher than that in BMMs or osteoblasts. *B*, intracellular ATP levels in BMMs, osteoclasts, and osteoblasts. Intracellular ATP levels in osteoclasts was markedly lower than not only osteoblasts, but also BMMs. *C*, effect of adenovirus-mediated expression of GFP (*AxGFP*; control), constitutively active MEK (*AxMEK^{CA}*), Bcl-2 (*AxBcl-2*), Bcl-x_L (*AxBcl-x_L*), or kinase-dead Csk (*AxCsk^{KD}*) on intracellular ATP levels in osteoclasts. Intracellular ATP levels in osteoclasts increased dramatically upon Bcl-x_L expression. *D* and *E*, real-time PCR analysis of *Bcl-x_L* mRNA level (*D*) and expression of Bcl-x_L protein (*E*) in BMMs and osteoclasts. Both mRNA and protein expression levels of Bcl-x_L in mature osteoclasts were markedly lower than in BMMs. *F*, effect of RANKL stimulation on expression level of Bcl-x_L in BMMs. Bcl-x_L expression level in BMMs was gradually reduced by RANKL stimulation. *G*, effect of retrovirus-mediated expression of small hairpin RNA targeting Bcl-x_L (*RxshBcl-x_L*) or Bcl-x_L (*RxBcl-x_L*) on NFATc1 protein levels in BMMs stimulated with RANKL. Increase and decrease in the expression level of NFATc1 were observed in shBcl-x_L and Bcl-x_L transfectants, respectively. *RxCtrl* indicates an empty retroviral control vector. *H*, osteoclast differentiation from BMMs infected with RxCtrl, RxshBcl-x_L, or RxBcl-x_L in response to RANKL and M-CSF. Cells were stained to evaluate TRAP-positive multinucleated osteoclast formation. *Scale bar*: 100 μm. *, $p < 0.05$, **, $p < 0.01$.

ings indicate that a decline in intracellular ATP stores with an increase in mitochondrial mass occurs during osteoclast differentiation through an unknown mechanism.

Possible Involvement of RANKL-induced Bcl-x_L Down-regulation in ATP Depletion and Osteoclast Maturation—The anti-apoptotic protein Bcl-x_L has been reported to regulate mitochondrial energetics through its interaction with the F_1F_O ATP synthase, which synthesizes ATP in the mitochondrial matrix using cytosolic ADP and phosphate as substrates (28, 29). In addition, we previously reported that overexpression of Bcl-x_L, Bcl-2, and constitutively active MEK (MEK^{CA}) strongly promotes osteoclast survival, and kinase-dead Csk (Csk^{KD}) expression increases Src kinase activity and bone-resorbing activity in osteoclasts (5, 21, 30, 31). The above mentioned data prompted us to measure total intracellular ATP levels in osteoclasts expressing these molecules. No differences in total intracellular ATP were observed among osteoclasts expressing MEK^{CA}, Bcl-2, or Csk^{KD}. However, intracellular ATP levels in oste-

oclasts increased more than 9-fold upon Bcl-x_L expression (Fig. 1*C*).

To elucidate the roles of intracellular ATP levels and Bcl-x_L expression in osteoclastogenesis, we evaluated Bcl-x_L expression in osteoclast lineage. Both Bcl-x_L mRNA and protein expression levels in mature osteoclasts were markedly lower than BMMs (Fig. 1, *D* and *E*). In addition, their expression levels in BMMs were gradually reduced by RANKL stimulation (Fig. 1*F*). Knockdown of the *Bcl-x* gene through RNAi promoted osteoclast differentiation upon RANKL stimulation, in line with an increase in the expression level of NFATc1, the key transcription factor of osteoclastogenesis (32). On the other hand, Bcl-x_L overexpression delayed the induction of NFATc1 by RANKL, which paralleled the reduced number of TRAP-positive multinucleated osteoclasts (Fig. 1, *G* and *H*). There was no significant difference in M-CSF-dependent proliferation of precursor cells (data not shown). Collectively, these data strongly indicate that lower cellular ATP levels associated with decreased expression of Bcl-x_L are important for osteoclast maturation.

Osteoclast-specific Tfam Knock-out Mice Exhibit Growth Retardation with Reduced Osteoclast Number—To investigate the role of intracellular ATP levels in osteoclast function in further detail, we generated osteoclast-specific *Tfam* conditional knock-out mice by mating $Tfam^{flox/flox}$ mice (13) with cathepsin K-Cre transgenic mice, in which the Cre recombinase gene was inserted into the cathepsin K locus and specifically expressed in osteoclasts (18). Tfam is ubiquitously expressed and absolutely required for mtDNA transcription. Loss of Tfam causes depletion of mtDNA, severe respiratory chain deficiency, and reduced ATP production (8, 13). The resulting cathepsin K-$Cre^{+/-}$ $Tfam^{flox/flox}$ mice (referred to herein as *Tfam* cKO mice) were born alive at predicted Mendelian frequencies. Tfam was markedly reduced in osteoclasts from *Tfam* cKO mice, whereas its expression in osteoblasts (Fig. 2*A*) and other tissues (data not shown) in *Tfam* cKO mice was comparable with that found in normal cathepsin K-$Cre^{-/-}$ $Tfam^{flox/flox}$ littermates.

An obvious feature of the 8-week-old male *Tfam* cKO mice was their reduced body size (Fig. 2*B*). Femoral length in male *Tfam* cKO mice was shorter when compared with $Tfam^{flox/flox}$ mice (13.29 ± 0.09 *versus* 15.31 ± 0.12 mm, $p < 0.01$; Fig. 2*C*). One year after birth, *Tfam* cKO mice were also significantly smaller than $Tfam^{flox/flox}$ mice (data not shown). Because Winkeler *et al.* (33) reported that cathepsin K is expressed in the testis, we evaluated testosterone levels in male *Tfam* cKO mice. We could not find any significant difference in serum testosterone levels between *Tfam* cKO mice and $Tfam^{flox/flox}$ mice (supplemental Fig. S1). Radiographic and microcomputed tomography analysis showed that there was no significant difference in bone mass between male *Tfam* cKO mice and $Tfam^{flox/flox}$ mice (Fig. 2, *C* and *D*). Interestingly, the number of TRAP-positive differentiated osteoclasts was dramatically reduced in *Tfam* cKO mice (Fig. 2, *E* and *F*). Despite similar expression levels of Tfam in $Tfam^{flox/flox}$ and *Tfam* cKO osteoblasts (Fig. 2*A*), some parameters of osteoblastic bone formation were also decreased in *Tfam* cKO mice (Fig. 2*G*). This attenuated osteoblast function may be due to the osteoclast-osteoblast coupling mechanism and contribute to the growth retardation observed in *Tfam* cKO mice.

ATP-depleted Tfam cKO Osteoclasts Show Increased Bone-resorbing Activity despite Accelerated Apoptosis—Unexpectedly, bone histomorphometric analysis showed that eroded surface per osteoclast (ES/Oc.N) was increased by *Tfam* ablation (Fig. 2*F*), indicating that *Tfam* cKO osteoclasts resorb bone more efficiently. To further investigate the influence of *Tfam* deficiency, osteoclasts were analyzed by electron microscopy using $Tfam^{flox/flox}$ and *Tfam* cKO mouse femurs. The results revealed that the normal ruffled border and sealing zone were clearly formed and faced the bone surface in *Tfam* cKO osteoclasts (data not shown). However, mitochondria of *Tfam* cKO osteoclasts appeared to exhibit disarray of mitochondrial cristae (Fig. 3*A*), suggestive of mitochondrial dysfunction. Given the mitochondrial morphological change in *Tfam* cKO mice, we analyzed the effect of *Tfam* deficiency on mitochondrial protein content and mtDNA levels in osteoclasts. As shown in Fig. 3*B*, mitochondrial protein content was slightly but significantly reduced by *Tfam* deficiency. Remarkably, we found that *Tfam* cKO osteoclasts contained only ~100 copies of mtDNA per nuclear genome, whereas control osteoclasts contained ~400 copies of mtDNA per nuclear genome (Fig. 3*C*). Consistent with these results, intracellular ATP levels in *Tfam* cKO osteoclasts were also significantly decreased when compared with $Tfam^{flox/flox}$ osteoclasts (Fig. 3*D*).

Because massive apoptosis in *Tfam* knock-out embryos was reported at embryonic day 9.5 and increased apoptosis in the heart of the tissue-specific *Tfam* knockouts was previously reported (13, 34), we next examined the role of Tfam in osteoclast survival. Mature osteoclasts undergo spontaneous apoptosis without any cytokines or supporting cells (3). After the removal of M-CSF and RANKL, ~80% of normal $Tfam^{flox/flox}$ osteoclasts died spontaneously within 24 h (Fig. 3*E*). ATP-depleted *Tfam* cKO osteoclasts disappeared more rapidly and exhibited a greater amount of cleaved caspase-3, a primary apoptosis executioner caspase, when compared with $Tfam^{flox/flox}$ osteoclasts, whereas *Tfam* deficiency increased bone-resorbing activity (Fig. 3, *E*–*G*), indicating a negative regulatory role of intracellular ATP levels in osteoclastic bone resorption. These results from our *in vitro* studies support our *in vivo* observations of decreased osteoclast number (Oc.N/BS) and increased eroded surface per osteoclast (ES/Oc.N) in *Tfam* cKO mice.

AMPK Activity Does Not Affect Osteoclast Survival and Bone Resorption—AMPK is a metabolic master switch that mediates the adaptation of the cell to variations in the nutritional environment (35). Its activity is stimulated by increases in the intracellular AMP/ATP ratio in response to stresses such as exercise, hypoxia, and glucose deprivation. Because the role of AMPK in osteoclast function has remained unexplored, we examined whether intracellular ATP levels affect AMPK activity in osteoclasts. As assessed by Western blotting, the phosphorylation level of AMPKα at Thr-172 at the activating loop was up-regulated in ATP-depleted osteoclasts after differentiation or *Tfam* ablation, whereas ATP-replete osteoclasts expressing Bcl-x_L exhibited lower AMPK phosphorylation (Fig. 4*A*). To test whether modulating AMPK activity would affect osteoclast

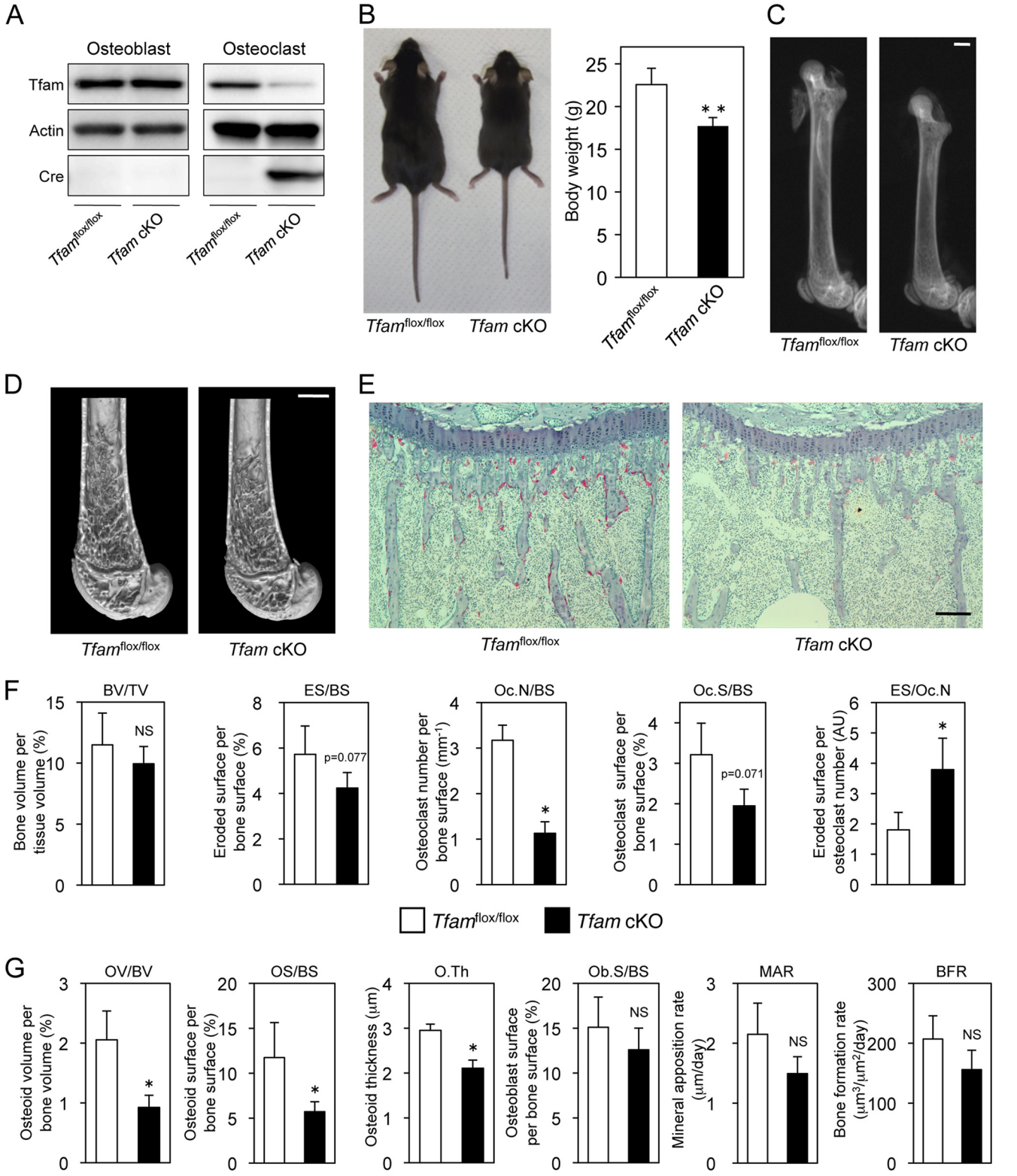

FIGURE 2. **Generation and skeletal analysis of *Tfam* cKO mice.** *A*, expression of Tfam, actin, and Cre proteins in osteoblasts and osteoclasts derived from *Tfam* cKO mice and their normal *Tfam*$^{flox/flox}$ littermates. Tfam was markedly reduced in osteoclasts derived from *Tfam* cKO mice. *B*, representative photographs and body weight of male *Tfam* cKO mice and their normal *Tfam*$^{flox/flox}$ littermates at 8 weeks of age. *C* and *D*, representative radiography images of the femur (*C*) and distal femur microcomputed tomography (*D*) of male *Tfam* cKO mice and their normal *Tfam*$^{flox/flox}$ littermates at 8 weeks of age. *Scale bar*: 1000 μm. *E*, histological analysis of proximal tibia of male *Tfam* cKO mice and their normal *Tfam*$^{flox/flox}$ littermates at 8 weeks of age (TRAP/hematoxylin staining). The number of TRAP-positive cells is markedly decreased in *Tfam* cKO mice. *Scale bar*: 100 μm. *F*, bone volume and parameters for osteoclastic bone resorption in the bone morphometric analysis of male *Tfam* cKO mice and their normal *Tfam*$^{flox/flox}$ littermates at 8 weeks of age ($n = 5$ for each genotype). Eroded surface per osteoclast (ES/Oc.N) was increased by *Tfam* ablation. *NS*, not significant; *AU*, arbitrary units. *G*, parameters for osteoblastic bone formation in the bone morphometric analysis of male *Tfam* cKO mice and their normal *Tfam*$^{flox/flox}$ littermates at 8 weeks of age ($n = 5$ for each genotype). *, $p < 0.05$, **, $p < 0.01$ *versus* normal *Tfam*$^{flox/flox}$ littermates.

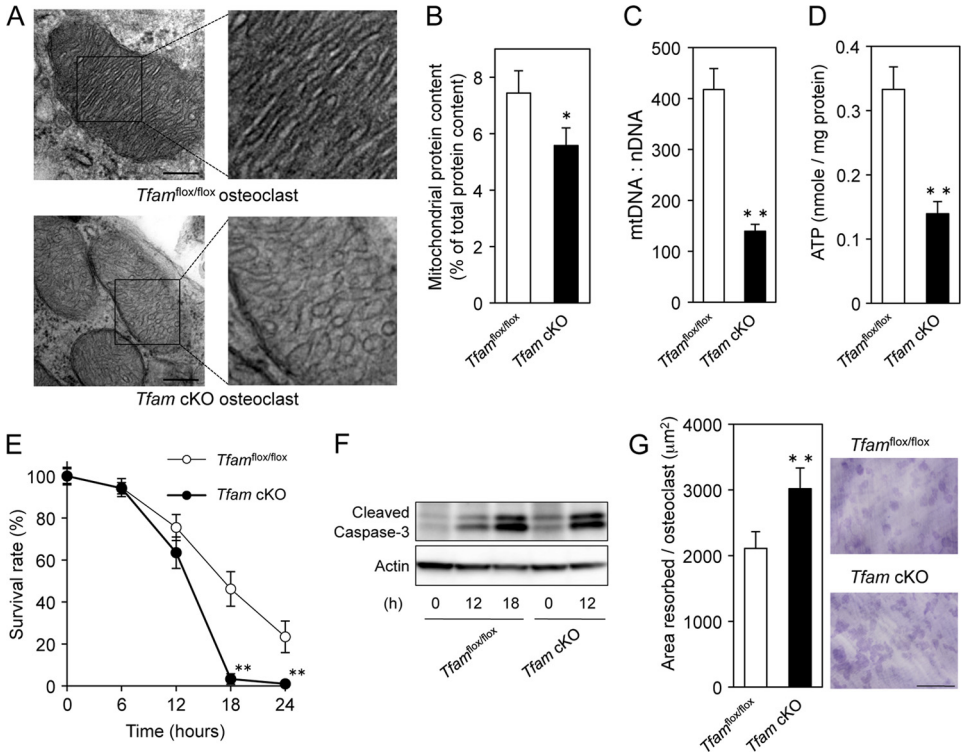

FIGURE 3. ***Tfam* cKO osteoclasts show increased bone-resorbing activity despite accelerated apoptosis.** *A*, electron microscopy of osteoclasts derived from *Tfam*$^{flox/flox}$ and *Tfam* cKO mice. Mitochondria in *Tfam* cKO osteoclasts appeared to display abnormal internal compartmentalization. Higher magnification images of the framed areas are shown in the *right panels*. Swollen and disorganized cristae were observed in *Tfam* cKO osteoclasts. *Scale bar*: 100 nm. *B*, mitochondrial protein content in *Tfam*$^{flox/flox}$ and *Tfam* cKO osteoclasts. Mitochondrial protein content was slightly but significantly reduced by *Tfam* deficiency. *C*, mtDNA copy number in *Tfam*$^{flox/flox}$ and *Tfam* cKO osteoclasts. mtDNA copy number per nuclear genome in osteoclasts was quantitated as described under "Experimental Procedures." Genotypes are indicated. *D*, intracellular ATP levels in *Tfam*$^{flox/flox}$ and *Tfam* cKO osteoclasts. Intracellular ATP levels in *Tfam* cKO osteoclasts were significantly decreased when compared with *Tfam*$^{flox/flox}$ osteoclasts. *E*, time course of the survival of *Tfam*$^{flox/flox}$ and *Tfam* cKO osteoclasts. The number of TRAP-positive viable cells remaining at the different time points is shown as a percentage of the cells at time 0. The survival rate of *Tfam* cKO osteoclasts was significantly lower than *Tfam*$^{flox/flox}$ osteoclasts. *F*, Western blotting of cleaved caspase-3 using β-actin as an internal control. *Tfam* cKO osteoclasts exhibited the increased amount of cleaved caspase-3. *G*, bone-resorbing activity of *Tfam*$^{flox/flox}$ and *Tfam* cKO osteoclasts. After transfer onto dentine slices, osteoclasts were further incubated for 12 h. The resorption pits were visualized by staining with 1% toluidine blue, and the resorbed area was quantified using an image analysis system. The pit-forming activity of *Tfam* cKO osteoclasts was significantly higher than that of *Tfam*$^{flox/flox}$ osteoclasts. Representative resorption pits, visualized by toluidine blue staining, are also shown. *Scale bar*: 500 μm. *, $p < 0.05$, **, $p < 0.01$ *versus* normal *Tfam*$^{flox/flox}$ osteoclasts.

function, we used adenovirus vectors containing dominant negative ($\alpha1^{DN}$, $\alpha2^{DN}$) or constitutively active ($\alpha1^{CA}$, $\alpha2^{CA}$) forms of AMPK catalytic subunits (α1 and α2). The expression of AMPK$\alpha1^{DN}$, AMPK$\alpha2^{DN}$, AMPK$\alpha1^{CA}$, and AMPK$\alpha2^{CA}$ was detected by immunoblotting using an antibody against the Myc tag. Because AMPK$\alpha1^{CA}$ and AMPK$\alpha2^{CA}$ are truncated mutants (Fig. 4*B*), they were detected as bands at a smaller molecular weight than AMPK$\alpha1^{DN}$ and AMPK$\alpha2^{DN}$ (Fig. 4*C*, *third panel*). As shown in Fig. 4*C*, *top panel*, the phosphorylation level of acetyl-CoA carboxylase at Ser-79, a direct target of AMPK, was modulated by adenovirus-mediated expression of the AMPK mutants. Modulation of AMPK activity did not affect osteoclast survival or bone resorption (Fig. 4, *D* and *E*), indicating that AMPK is not involved in ATP depletion-induced bone resorption.

Extracellular ATP Inhibits Osteoclast Function—The release of ATP has been reported in a variety of cell types (6, 7, 36). To determine whether intracellular ATP levels influence constitutive ATP release from osteoclasts, extracellular ATP concentrations were measured. ATP release from ATP-depleted *Tfam* cKO osteoclasts was significantly reduced when compared with *Tfam*$^{flox/flox}$ osteoclasts, whereas Bcl-x_L overexpression had the opposite effect (Fig. 5*A*). Although detailed molecular mechanisms for the release of cellular ATP have remained largely elusive, the increased ATP release appeared to occur as a result of higher intracellular ATP concentrations. We next examined the effect of extracellular ATP on osteoclast function. To avoid rapid hydrolysis of ATP by ectonucleotidases, we used the hydrolysis-resistant ATP analogue, ATPγS (37). As shown in Fig. 5*B*, the addition of 100 μM ATPγS dramatically reduced osteoclast survival and bone resorption. Interestingly, after stimulation with 100 μM ATPγS for 3 h, most of the osteoclasts exhibited a large vacuole formation (Fig. 5*C*, *middle panel*). Because membrane blebs or vacuoles are a typical feature of ATP-stimulated cells and are mainly caused by stimulation of the P2X7 receptor (38), we also examined the effect of BzATP, a relatively potent P2X7 agonist, on osteoclast function. Treatment with 150 μM BzATP for 30 min caused dramatic changes in osteoclast morphology with numerous large cytoplasmic vacuoles (Fig. 5*C*, *bottom panel*). Osteoclast survival and bone-resorbing activity were also strongly inhibited in the presence of 150 μM BzATP (Fig. 5*B*), suggesting that extracellular ATP may have inhibitory effects on morphology, survival, and the bone-resorbing activity of mature osteoclasts.

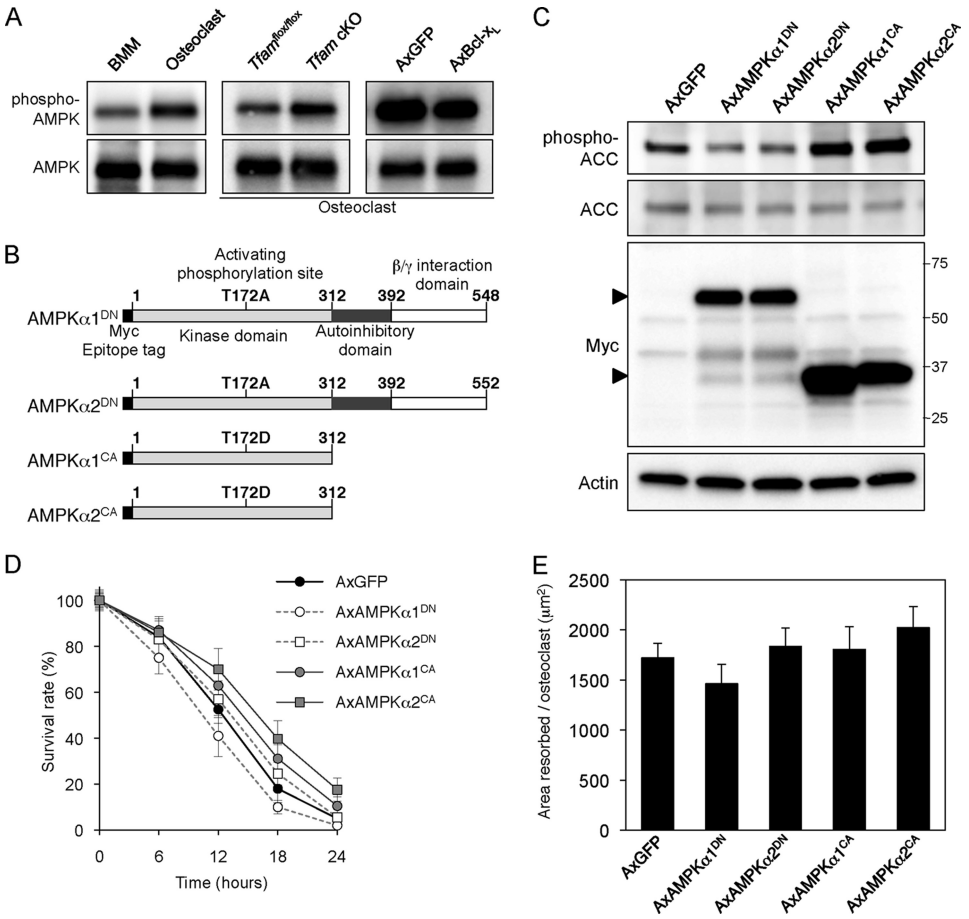

FIGURE 4. **AMPK activity does not affect osteoclast function.** *A*, effect of intracellular ATP level on AMPK activity. Basal activity of AMPK was up-regulated in ATP-depleted osteoclasts after differentiation (*left panel*) or *Tfam* ablation (*middle panel*), whereas ATP-replete osteoclasts expressing Bcl-x_L exhibited lower AMPK phosphorylation (*right panel*). *AxGFP*, adenovirus-mediated expression of GFP; *AxBcl-x$_L$*, adenovirus-mediated expression of Bcl-x_L. *B*, schematic representation of AMPK$\alpha1^{DN}$, AMPK$\alpha2^{DN}$, AMPK$\alpha1^{CA}$, and AMPK$\alpha2^{CA}$. *C*, adenovirus-mediated expression of AMPK mutants (*AxAMPK*) and modulation of AMPK activity in osteoclasts. The phosphorylation level of acetyl-CoA carboxylase (*ACC*) at Ser-79, a direct target of AMPK, was reduced by adenovirus-mediated expression of AMPK$\alpha1^{DN}$ or AMPK$\alpha2^{DN}$, whereas induction of AMPK$\alpha1^{CA}$ or AMPK$\alpha2^{CA}$ dramatically increased acetyl-CoA carboxylase phosphorylation. *D*, time course of survival of osteoclasts expressing AMPK mutants. The number of TRAP-positive viable cells remaining at the different time points is shown as a percentage of the cells at time 0. Modulation of AMPK activity did not appear to affect osteoclast survival. *E*, bone-resorbing activity of osteoclasts expressing AMPK mutants. After transfer onto dentine slices, osteoclasts were further incubated for 12 h. No differences in the bone-resorbing activity were observed among osteoclasts expressing AMPK mutants.

The Inhibitory Effect of Extracellular ATP on Osteoclast Survival, but Not on Bone-resorbing Activity, Is Rescued by Bcl-x_L-induced ATP Repletion—Because intracellular and extracellular ATP affect osteoclast apoptosis in opposite ways, we examined the consequences induced by intra- and extracellular ATP in the regulation of osteoclast survival. ATP repletion by Bcl-x_L expression completely reversed the inhibitory effect of ATPγS on osteoclast survival (Fig. 6*A*, *left*). In addition, the overall survival curve of Bcl-x_L-expressing osteoclasts showed a 30% reduction during the first 6 h after BzATP addition, after which stabilization occurred (Fig. 6*A*, *right*), suggesting that intracellular ATP may be more important than extracellular ATP in regulating osteoclast survival. Although Bcl-x_L expression itself has an inhibitory effect on bone resorption (5), bone-resorbing activity of osteoclasts expressing Bcl-x_L was significantly further inhibited by treatments with ATPγS or BzATP (Fig. 6*B*) despite the improvement of survival rate, thereby confirming that extracellular ATP has a clear inhibitory effect on osteoclastic bone resorption.

Extracellular ATP Alters the Pattern of Pyk2 Distribution in Osteoclasts—Following ATP stimulation, the 240-kDa membrane-associated cytoskeletal protein, α-fodrin, which is important for maintaining normal membrane structure and supporting cell surface protein function, was reported to be cleaved into smaller fragments, including 180, 150, and 120 kDa (39). In addition, α-fodrin degradation is proposed to contribute to cell blebbing and other morphologic changes (40). Extracellular ATP stimulation is also reported to induce c-Src activation and tyrosine phosphorylation of intracellular proteins (41, 42). However, we could not detect degradation in cytoskeletal proteins including α-fodrin, actin, c-Src, and Pyk2. Tyrosine-phosphorylated protein patterns remained unchanged upon ATPγS or BzATP stimulation (Fig. 7*A*). Due to dramatic morphological changes after stimulation with the ATP analogues (Fig. 5*C*), we further examined the effect of extracellular ATP on osteoclast actin cytoskeleton using confocal microscopy. Although the actin ring, which is a characteristic of polarized osteoclasts, was clearly formed before ATP stimulation,

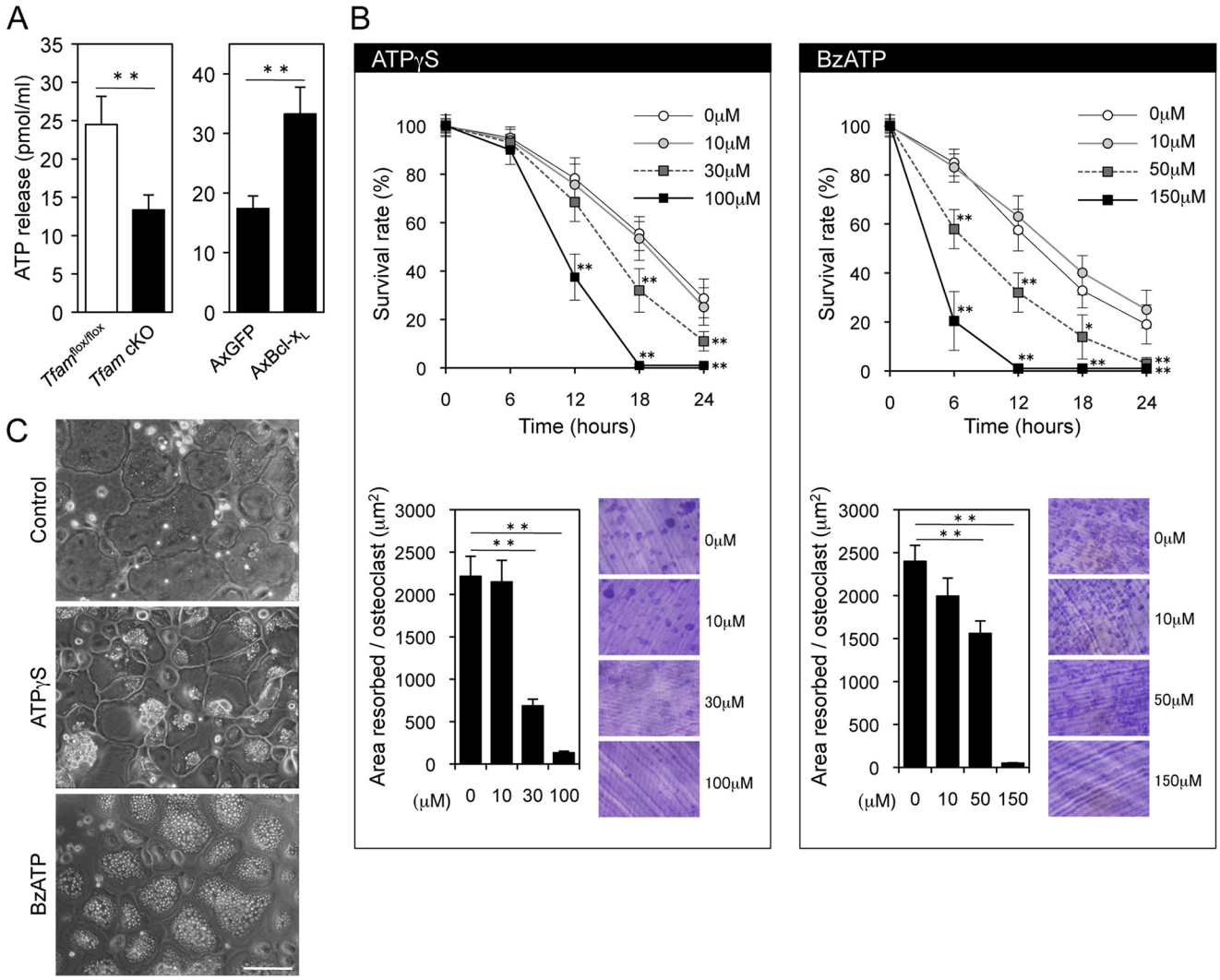

FIGURE 5. **Extracellular ATP inhibits osteoclast function.** *A*, the effects of intracellular ATP levels on constitutive ATP release. ATP release from ATP-depleted *Tfam* cKO osteoclasts was reduced (*left panel*), whereas ATP-replete osteoclasts expressing Bcl-x_L showed enhanced basal ATP release (*right panel*). **, $p < 0.01$. *AxGFP*, adenovirus-mediated expression of GFP; *AxBcl-x$_L$*, adenovirus-mediated expression of Bcl-x_L. *B*, the effects of ATPγS (*left panel*) and BzATP (*right panel*) on the survival and bone-resorbing activity of osteoclasts. The addition of ATPγS and BzATP dramatically reduced osteoclast survival and bone resorption in a dose-dependent manner. *, $p < 0.05$, **, $p < 0.01$ *versus* untreated osteoclasts. *C*, morphological changes in osteoclasts stimulated with 100 μM ATPγS for 3 h (*middle panel*) or 150 μM BzATP for 30 min (*bottom panel*). The treatment with these ATP analogues caused morphological changes with numerous cytoplasmic vacuoles. *Scale bar*: 100 μm.

ATPγS- or BzATP-treated osteoclasts exhibited diffuse actin distribution (Fig. 7*B*). Interestingly, stimulation with ATPγS or BzATP facilitated translocation of Pyk2, a major adhesion-dependent tyrosine kinase in osteoclasts, from the periphery to the cell center (Fig. 7*B*). We obtained similar results using a biochemical method with Triton-insoluble cytoskeletons of osteoclasts. The amount of Pyk2 that remained associated with the cytoskeletons was reduced after treatment with ATPγS or BzATP (Fig. 7*C*), indicating that the inhibitory effect of extracellular ATP on bone resorption was due to altered cytoskeletal structures.

Bone-resorbing Activity Is Up-regulated by Removal of Extracellular ATP or P2X7 Receptor Blockade—The lifetime of released ATP is short due to the presence of ecto-ATPase. To explore the physiological role of released cellular ATP, we analyzed the effect of apyrase, which hydrolyzes ATP, on osteoclast function. As shown in Fig. 8*A*, removal of extracellular ATP with apyrase up-regulated osteoclastic bone resorption with a slight increase in osteoclast survival. We next examined how P2X7 receptor blockade affects osteoclast function. Although Pellegatti *et al.* (43) reported that the P2X7 receptor drives fusion of M-CSF/RANKL-stimulated monocytes into multinucleated osteoclasts, *P2rx7*$^{-/-}$ mice exhibited a significant decrease in bone mass associated with an increased number of osteoclasts per bone surface (Oc.N/BS) (19). Because it is possible that the findings related to bone resorption in *P2rx7*$^{-/-}$ mice may be caused by alteration in other cell types that regulate osteoclast function, survival and pit formation assays were performed using osteoclasts derived from *P2rx7*$^{-/-}$ and *P2rx7*$^{+/+}$ mice. *P2rx7* deficiency increased osteoclastic bone resorption with a tendency toward increased survival (Fig. 8*B*). Together, these results strongly suggest that physiological concentrations of extracellular ATP can exert a negative impact on osteoclast bone-resorbing activity via purinergic receptors.

Intracellular ATP Affects Bone-resorbing Activity via Released Cellular ATP—To further confirm whether ATP release from intracellular stores affects osteoclast function,

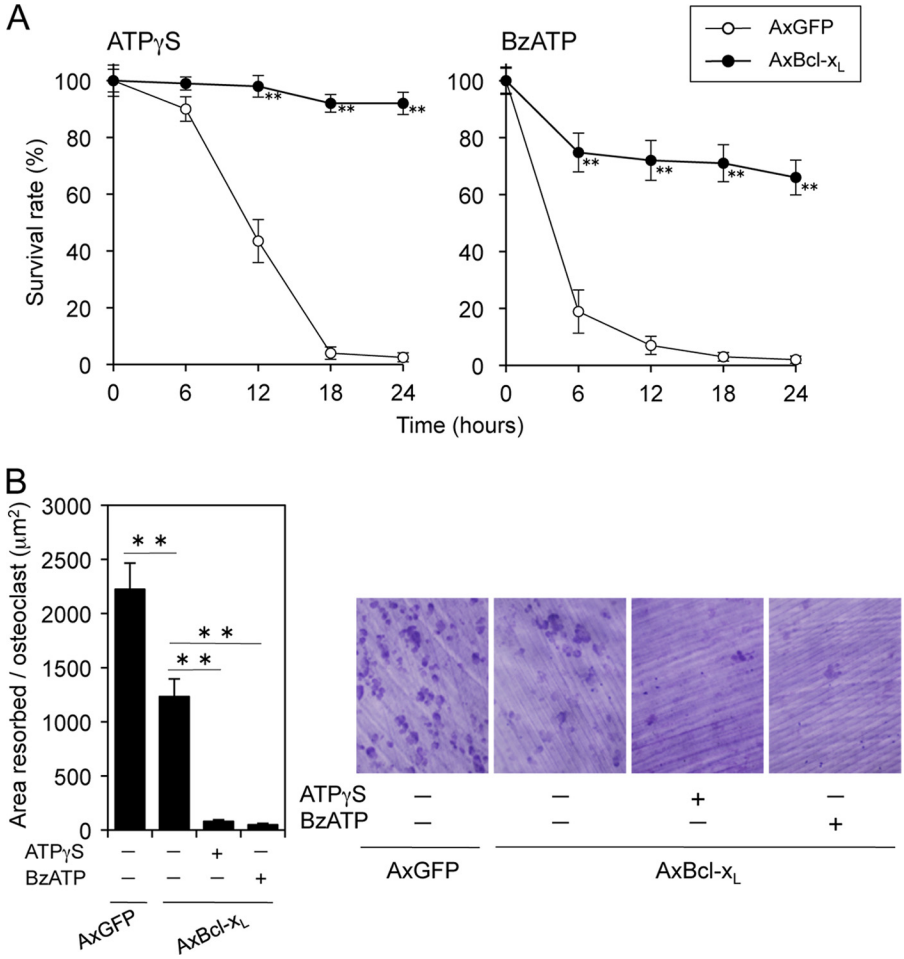

FIGURE 6. **Adenovirus-mediated Bcl-x_L (*AxBcl-x_L*) infection reversed the inhibitory effect of extracellular ATP on osteoclast survival but not on bone-resorbing activity.** *A*, time course of the survival of Bcl-x_L-expressing osteoclasts treated with 100 μM ATPγS or 150 μM BzATP. Bcl-x_L expression completely reversed the inhibitory effect of ATPγS on osteoclast survival, whereas the survival curve of Bcl-x_L-expressing osteoclasts showed a 30% reduction during the first 6 h after BzATP addition, after which stabilization occurred. **, $p < 0.01$ *versus* adenovirus-mediated expression of GFP (*AxGFP*)-infected osteoclasts. *B*, bone-resorbing activity of Bcl-x_L-expressing osteoclasts treated with 100 μM ATPγS or 150 μM BzATP. Bone-resorbing activity of osteoclasts expressing Bcl-x_L was significantly inhibited by treatments with ATPγS or BzATP, despite the improvement of survival rate. Representative resorption pits, visualized by toluidine blue staining, are also shown. **, $p < 0.01$.

we selected Bcl-x_L-overexpressing osteoclasts as a model system, which showed increased release of cellular ATP (Fig. 5*A*). Even after 48 h, >85% of Bcl-x_L-overexpressing osteoclasts were still alive (data not shown). In addition, after a 48-h incubation, most of these cells exhibited large vacuoles and membrane blebs (Fig. 8*C*, *left panel*), possibly through continuous exposure to locally high ATP in the immediate vicinity of cell surfaces. Furthermore, these dramatic morphological changes were reduced by apyrase treatment or *P2rx7* ablation (Fig. 8*C*, *middle* and *right panels*). Consistent with these results, the inhibitory effect of Bcl-x_L expression on osteoclastic bone resorption was partially reversed by apyrase or *P2rx7* deficiency (Fig. 8*D*). These results strongly support our hypothesis that the release of ATP from intracellular stores and autocrine/paracrine feedback through purinergic receptors control the bone-resorbing activity of mature osteoclasts.

Osteoclasts Derived from Aged Mice Display ATP Depletion with Increased Bone-resorbing Activity—mtDNA deletions, mutations, and reduction have been reported to occur with aging in various tissues (44, 45). To determine the functional impact of these changes, we measured mtDNA copy number in osteoclasts derived from 3- and 24-month-old mice. For the old group, 24-month-old mice were used because C57BL/6 mice were already reported to lose bone continuously to 24 months of age (46). As shown in Fig. 9*A*, mtDNA copy number was significantly reduced without changing mitochondrial protein content in the osteoclasts of 24-month-old mice (supplemental Fig. S2*A*). Although the expression levels of *Bcl-x_L* and *Tfam* remained unchanged with aging (supplemental Fig. S2*B*), intracellular ATP levels were significantly decreased in the osteoclasts of 24-month-old mice (Fig. 9*B*). As shown in Fig. 9, *C* and *D*, these osteoclasts exhibited increased bone resorption with a tendency toward shorter survival. Furthermore, real-time RT-PCR analysis suggested that the expression level of *P2rx7* in osteoclasts was dramatically decreased when compared with BMMs (supplemental Fig. S3*A*). These results indicate that the reduction of *P2rx7* expression during osteoclastogenesis, which led to a decreased response to external ATP, may contribute to up-regulation of bone-resorbing activity. However, we could not detect any difference in the expression level of *P2rx7* in osteoclasts derived from 3- and 24-month-

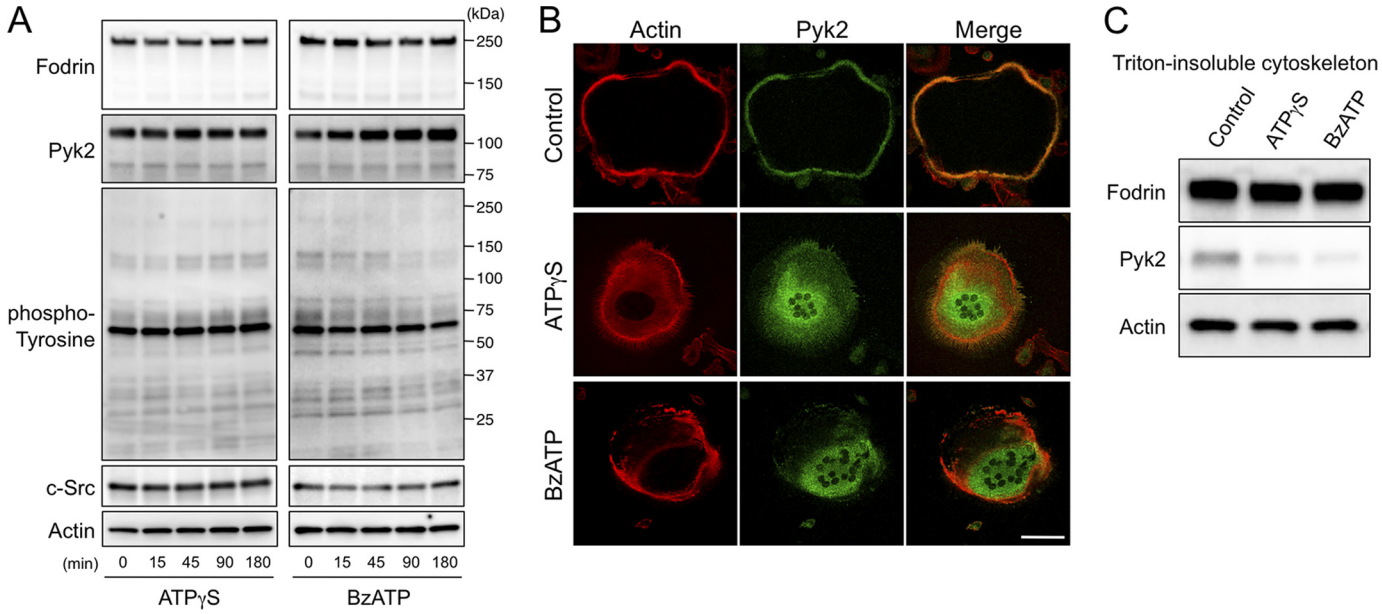

FIGURE 7. **Extracellular ATP alters Pyk2 distribution in osteoclasts.** *A*, Western blot analysis of fodrin, Pyk2, phospho-tyrosine, c-Src, and actin levels in osteoclasts treated with ATPγS or BzATP at different time points. Degradation in cytoskeletal proteins including α-fodrin, actin, Pyk2, and c-Src was not detected, and tyrosine-phosphorylated protein patterns remained unchanged upon ATPγS (100 μM) or BzATP (150 μM) stimulation. *B*, double immunofluorescence staining of F-actin (*red*) and Pyk2 (*green*) in osteoclasts after stimulation of ATPγS (100 μM) or BzATP (150 μM) for 1 h. Stimulation with ATPγS or BzATP disrupted the actin ring formation of osteoclasts and facilitated translocation of Pyk2 from the periphery to the cell center. *Scale bar*: 50 μm. *C*, Western blots of Triton X-100-insoluble cytoskeletons of osteoclasts treated with ATPγS (100 μM) or BzATP (150 μM) for 1 h. Note that the amount of Pyk2 stayed associated with the cytoskeletons was reduced after ATPγS or BzATP stimulation.

old mice (supplemental Fig. S3*B*), suggesting that age-related changes in bone-resorbing activity may be due to the decrease in mtDNA copy number and intracellular ATP, not to altered responses to extracellular ATP by aging. These results confirmed our findings that ATP depletion leads to osteoclastic bone resorption.

DISCUSSION

The finding that bisphosphonates directly inhibit osteoclast survival has attracted a great deal of attention to the molecular mechanism of osteoclast apoptosis, and remarkable progress has been made in the last 10 years to reveal the signaling pathways involved in the process. Recently, it was reported that nitrogen-containing bisphosphonate risedronate induces osteoclast apoptosis through the mitochondria-dependent pathway with an increased expression of Bim, a proapoptotic BH3-only Bcl-2 family member, and that the proapoptotic effect of risedronate is suppressed by *Bim* deletion (47). Interestingly, $Bim^{-/-}$ osteoclasts showed decreased bone-resorbing activity despite prolonged survival (4). In contrast, osteoclasts lacking antiapoptotic Bcl-x_L exhibited the opposite pattern, namely, increased bone resorption with accelerated apoptosis (5), indicating that there may be an inverse correlation between osteoclast survival *versus* bone resorption. This negative relationship was also observed in *Tfam* cKO osteoclasts. Taken together, it is likely that osteoclasts complete their work at the sacrifice of their health.

Without ATP, life as we understand it could not exist. Even bacteria rely on an ATP molecule identical to that used in humans. One of the primary goals of the present study was to determine whether numerous high-functioning mitochondria plentifully produce ATP in osteoclasts to meet the energy demands for bone resorption, or conversely, whether osteoclasts work very hard and ATP is used up during bone resorption. We demonstrate that mature osteoclasts were depleted of ATP content when compared with BMMs, indicating that they are likely to wear out. Low intracellular ATP levels favor the release of cytochrome *c*, resulting in high apoptotic rates (48). It is possible that the apoptosis-sensitive phonotype of mature osteoclasts may be partly caused by ATP down-regulation. In addition, severe ATP depletion following *Tfam* ablation accelerated osteoclast apoptosis, whereas higher intracellular ATP concentrations by Bcl-x_L expression promoted osteoclast survival and exceeded the negative effect of extracellular ATP, suggesting that intracellular ATP content is one of the key players in regulating osteoclast survival.

ATP depletion during osteoclastogenesis was found to be associated with RANKL-induced down-regulation of Bcl-x_L expression. Bcl-x_L overexpression failed to up-regulate osteoclastic bone resorption despite ameliorating ATP depletion. In contrast, ATP-depleted *Tfam* cKO osteoclasts showed increased bone resorption. This strange pattern of responses to intracellular ATP content suggests the existence of an unknown mechanism that regulates osteoclast bone-resorbing activity. One possible explanation for this strange pattern is that the metabolic stress-sensing protein kinase AMPK may play an important role in bone resorption. In fact, AMPK activity in osteoclasts was modulated in a manner opposite to intracellular ATP levels (Figs. 1, *B* and *C*, 3*D*, and 4*A*). However, changes in AMPK activity by adenovirus-mediated introduction of AMPK mutants failed to affect osteoclast survival and bone resorption. Another possible hypothesis is that released ATP from intracellular stores may have an inhibitory effect on

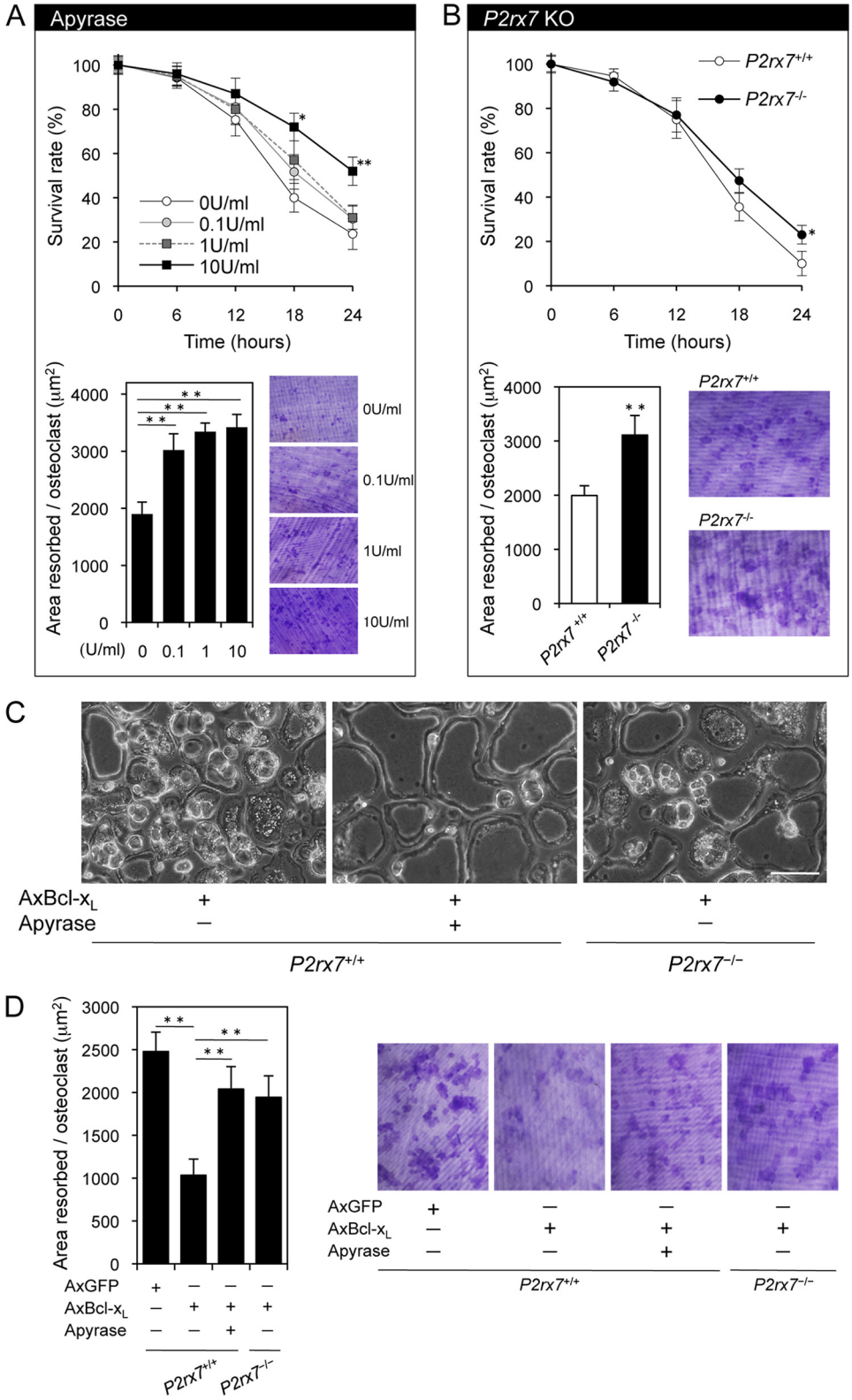

FIGURE 8. **Effects of removal of extracellular ATP or P2X7 receptor blockade on osteoclastic bone resorption.** *A*, the effects of apyrase, which hydrolyzes extracellular ATP, on the survival and bone-resorbing activity of osteoclasts. Apyrase treatment up-regulated osteoclastic bone resorption with a slight increase in osteoclast survival. *, $p < 0.05$, **, $p < 0.01$ *versus* untreated osteoclasts. *B*, the effects of *P2rx7* deficiency on the survival and bone-resorbing activity of osteoclasts. *P2rx7* deficiency increased osteoclastic bone resorption with a tendency toward increased survival. *, $p < 0.05$, **, $p < 0.01$ *versus* normal *P2rx7*$^{+/+}$ osteoclasts. *C*, morphological changes in Bcl-x_L-expressing osteoclasts after a 48-h incubation. Note that Bcl-x_L-induced morphological changes including large vacuoles and membrane blebs were reduced by apyrase treatment (10 units/ml) or *P2rx7* deficiency. *AxBcl-x$_L$*, adenovirus-mediated expression of Bcl-x_L. *Scale bar*: 100 μm. *D*, bone-resorbing activity of *P2rx7*$^{+/+}$ osteoclasts expressing Bcl-x_L treated with apyrase and *P2rx7*$^{-/-}$ osteoclasts expressing Bcl-x_L. The inhibitory effect of Bcl-x_L expression on osteoclastic bone resorption was partially reversed by apyrase (10 units/ml) or *P2rx7* deficiency. Representative resorption pits, visualized by toluidine blue staining, are also shown. *AxGFP*, adenovirus-mediated expression of GFP. **, $p < 0.01$.

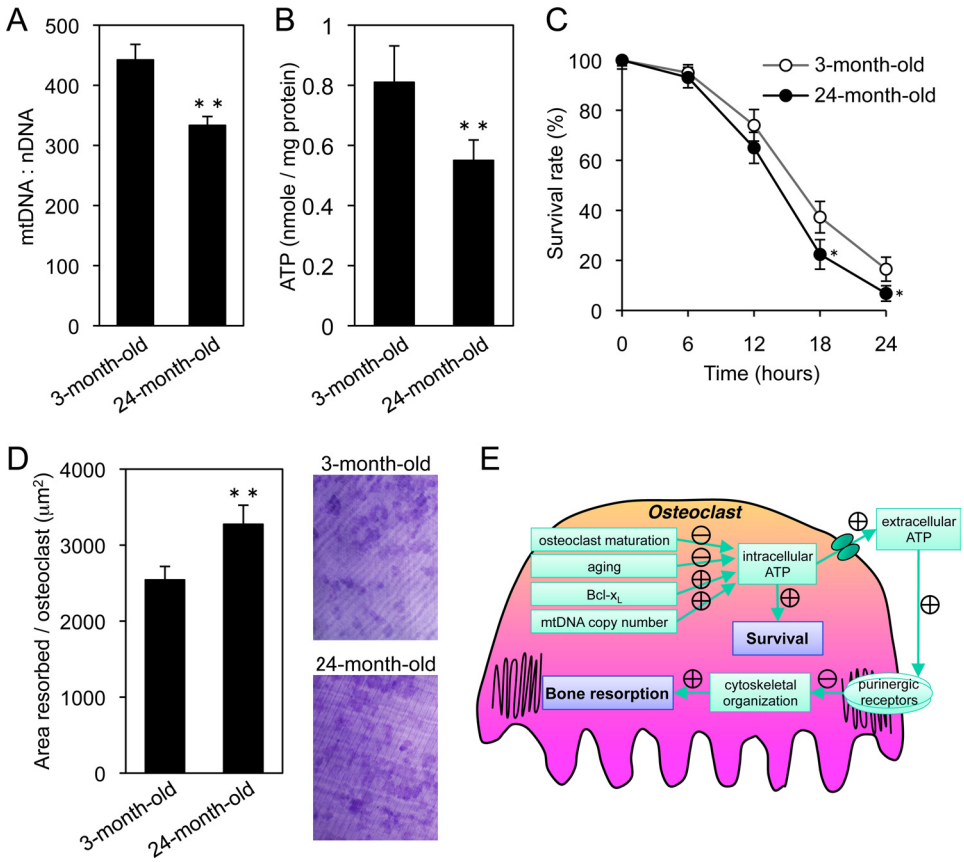

FIGURE 9. **Age-related changes in osteoclasts and a model for the role of intracellular ATP levels in osteoclastic bone resorption.** *A* and *B*, mtDNA copy number (*A*) and intracellular ATP levels (*B*) in osteoclasts derived from 3- and 24-month-old mice. mtDNA copy number and intracellular ATP levels were significantly decreased in the osteoclasts of 24-month-old mice. *C* and *D*, time course of the survival (*C*) and bone-resorbing activity of osteoclasts (*D*) derived from 3- and 24-month-old mice. The osteoclasts of 24-month-old mice exhibited increased bone resorption with a tendency toward shorter survival. Representative resorption pits, visualized by toluidine blue staining, are also shown. *E*, graphic showing how osteoclasts exhibit the inverse correlation between their survival and bone-resorbing activity. In osteoclasts, intracellular ATP levels is influenced by developmental, physiological, and pathological cues. Intracellular ATP content is one of the key players in regulating osteoclast survival. On the other hand, released ATP from intracellular stores has an inhibitory effect on cytoskeletal organization and osteoclastic bone resorption via purinergic receptors. The delicate functional balance of intracellular and extracellular ATP levels regulates osteoclast function. *, $p < 0.05$, **, $p < 0.01$ *versus* osteoclasts derived from 3-month-old mice.

osteoclastic bone resorption. First, we demonstrated that the steady-state level of extracellular ATP in cell cultures reflected intracellular ATP level in osteoclasts. Next, we found that high extracellular ATP concentrations strongly inhibited osteoclastic bone resorption. This inhibitory effect was caused by disruption of cytoskeletal organization including complete mislocalization of Pyk2 within cells. Pyk2 is reported to modulate integrin-dependent recruitment of cytoskeletal molecules that are important for adhesion, migration, and vesicular trafficking of mature osteoclast on bone (49), and *Pyk2*-null osteoclasts fail to form a podosome belt that is typically seen at the periphery of wild-type osteoclasts, resulting in a cell-autonomous defect in bone resorption (50). The above issues suggest that Pyk2 mislocalization following high extracellular ATP concentration is one of the biggest factors leading to defective bone resorption. Finally, we found that apyrase treatment or *P2rx7* ablation upregulated bone-resorbing activity. The direct functional link between intracellular ATP and osteoclastic bone resorption was clarified by our experiments with ATP-replete osteoclasts by Bcl-x_L expression, in which removal of extracellular ATP or ablation of P2X7 receptor reduced deteriorative morphological changes and partially reversed the inhibitory effect on bone resorption (Fig. 8, *C* and *D*). These findings suggest that mature osteoclasts with ATP depletion resorb bone efficiently with their normal cytoskeleton, even during their short lifespan (Fig. 9*E*).

Cytosolic ATP concentrations are high (~3 mM) and provide the source for extracellular ATP (51). The mechanism of nucleotide release from cells is currently not sufficiently understood. Recently, several mechanisms for ATP release from cells have been proposed, and they are activated by a wide range of stimuli (52, 53). These ATP release mechanisms include damage to the cell membrane, mechanical stress, hypoxia, inflammation, several agonists, and electrical excitation of neural tissue. In non-excitable cells, a number of possible cellular mechanisms for ATP release have been studied, including exocytosis, gap junction hemichannels, ion channels, the cystic fibrosis transmembrane conductance regulator, and nucleotide transporters. Several properties and findings make pannexin 1 a very attractive candidate for an ATP-releasing channel. Homomeric pannexin 1 hexamers do not form gap junctions when expressed in mammalian cells and, instead, operate as plasma membrane channels (54, 55). They are activated by mechanical stress, membrane depolarization, and in a receptor-dependent manner. Despite the potential role of these channels in ATP release in numerous cell types (56), it needs to be realized that the precise

mechanism of spontaneous constitutive ATP release remains unresolved and controversial.

Hazama *et al.* (57) reported that the treatment of 0.5 mM ATP or 300 μM BzATP increased bone resorption. In their experimental system, they used human osteoclasts, which are differentiated from CD14-positive monocyte on dentin slices under osteoclast-inducing condition for 3 weeks. In addition, their bone resorption assay is performed by counting the number of pits, not by measuring the pit area. In contrast to their results, we found that the pit area was dramatically decreased after treatment of 100 μM ATPγS or 150 μM BzATP on the bone-resorbing activity by measuring the pit area using mouse osteoclasts (Fig. 5*B*). In addition, removal of extracellular ATP with apyrase up-regulated osteoclastic bone resorption (Fig. 8*A*). It should also be noted that *P2rx7*$^{-/-}$ mice exhibited a significant decrease in bone mass associated with increased number of osteoclast per bone surface (19). This is consistent with our findings that extracellular ATP has a deteriorative effect on osteoclast function. We cannot fully explain the reason for the discrepancy between our results and those of the previous study, but it is possible that human osteoclasts have a different profile of functional P2X receptors and that counting the number of pits using human osteoclasts, which require 3 weeks of culture on dentin slices, may be inappropriate to investigate the bone-resorbing activity of mature osteoclasts *in vitro*.

Our *in vitro* study showed that *Tfam*-deficient osteoclasts exhibited increased bone-resorbing activity and decreased survival. Due to this contrary relationship, it is possible that *Tfam* cKO mice develop two different phenotypes; osteoporosis is one predicted consequence of increased bone-resorbing activity, and osteopetrosis is another consequence of a reduced number of osteoclasts. According to the bone histomorphometric analysis, Oc.N/BS was dramatically reduced, whereas ES/BS and Oc.S/BS (where Oc.S. indicates osteoclast surface) were also reduced with marginal statistical difference ($p < 0.1$) (Fig. 2*F*), indicating that overall bone resorption in *Tfam* cKO mice was slightly reduced. Because some parameters of osteoblastic bone formation decreased and several coupling factors were reported to be involved in osteoclast-mediated promotion of osteoblast recruitment and maturation (58), we investigated the expression levels of candidate coupling factors, such as Wnt10b, BMP6, and sphingosine kinase 1 (SPHK1) in *Tfam* cKO osteoclasts. However, we could not find any difference in these factors (data not shown). One possible explanation for the decrease in osteoblast parameters is that dramatically reduced number of osteoclasts may lead to a decrease in the concentration of osteoclast-derived coupling factors in the bone marrow microenvironment. On the other hand, ATP released from bone cells through constitutive and inducible mechanisms is reported to promote osteogenesis *in vitro* (59–61). Moreover, osteogenesis and anabolic responses to mechanical loading are impaired in *P2rx7*$^{-/-}$ mice (19, 62), indicating that release of ATP into the bone extracellular fluid occurs *in vivo*. It is also possible that the observed reduction in osteoblast parameters and body size in *Tfam* cKO mice may be caused by reduced release of ATP from *Tfam*-deficient osteoclasts. Together, the reduced number of osteoclasts and decreased amount of osteoclast-derived coupling factors following *Tfam* deficiency achieve a balance between bone resorption and formation, resulting in similar bone mass.

Osteoporosis, a classical age-related disease, is a systemic skeletal disease characterized by low bone mass and microarchitectural deterioration of bone tissue, with a consequent increase in bone fragility. Most studies evaluating age-related changes in bone resorption markers observed an increase in serum and urinary indices (63–66). mtDNA deletions, mutations, and reductions have been reported to occur with aging in various tissues (44, 45). The above issues suggest that mtDNA copy number may decrease with age in osteoclasts, which might in turn contribute to the age-related increase in bone resorption. Experiments using osteoclasts derived from 3- and 24-month-old mice showed that mtDNA copy number and intracellular ATP level decreased with age. In addition, we found a positive correlation between age and bone-resorbing activity of osteoclasts. These findings from aged osteoclasts confirm our findings that lower intracellular ATP levels up-regulate osteoclastic bone resorption. Age-related mitochondrial dysfunction, such as reduced mtDNA copy number, is likely to be involved in the development of osteoporosis.

In conclusion, the results of the present study demonstrate that intracellular ATP levels play a pivotal role, not only in osteoclast apoptosis, but also in the bone-resorbing function of the cells. Further investigation of mitochondrial functions regulating the inverse correlation between osteoclast survival and bone resorption will give new insights into the molecular mechanisms regulating bone homeostasis.

Acknowledgments—Tfam$^{flox/flox}$ *mice were kindly provided by Dr. Nils-Göran Larsson (Karolinska Institutet). Cathepsin K-Cre mice were kindly provided by Dr. Shigeaki Kato (University of Tokyo). We thank Yasuhiro Sawada (National University of Singapore), Shigeru Yamada, Sachiho Kubo, Daichi Fukunaga, Ryo Nakayama, and Naoya Murase (Tokyo Metropolitan Geriatric Hospital and Institute of Gerontology) for helpful discussion.*

REFERENCES

1. Boyle, W. J., Simonet, W. S., and Lacey, D. L. (2003) Osteoclast differentiation and activation. *Nature* **423,** 337–342
2. Negishi-Koga, T., and Takayanagi, H. (2009) Ca^{2+}-NFATc1 signaling is an essential axis of osteoclast differentiation. *Immunol. Rev.* **231,** 241–256
3. Tanaka, S., Miyazaki, T., Fukuda, A., Akiyama, T., Kadono, Y., Wakeyama, H., Kono, S., Hoshikawa, S., Nakamura, M., Ohshima, Y., Hikita, A., Nakamura, I., and Nakamura, K. (2006) Molecular mechanism of the life and death of the osteoclast. *Ann. N.Y. Acad. Sci.* **1068,** 180–186
4. Akiyama, T., Bouillet, P., Miyazaki, T., Kadono, Y., Chikuda, H., Chung, U. I., Fukuda, A., Hikita, A., Seto, H., Okada, T., Inaba, T., Sanjay, A., Baron, R., Kawaguchi, H., Oda, H., Nakamura, K., Strasser, A., and Tanaka, S. (2003) Regulation of osteoclast apoptosis by ubiquitylation of proapoptotic BH3-only Bcl-2 family member Bim. *EMBO J.* **22,** 6653–6664
5. Iwasawa, M., Miyazaki, T., Nagase, Y., Akiyama, T., Kadono, Y., Nakamura, M., Oshima, Y., Yasui, T., Matsumoto, T., Nakamura, T., Kato, S., Hennighausen, L., Nakamura, K., and Tanaka, S. (2009) The antiapoptotic protein Bcl-x_L negatively regulates the bone-resorbing activity of osteoclasts in mice. *J. Clin. Invest.* **119,** 3149–3159
6. Bodin, P., and Burnstock, G. (2001) Purinergic signaling: ATP release. *Neurochem. Res.* **26,** 959–969
7. Burnstock, G. (2002) Purinergic signaling and vascular cell proliferation and death. *Arterioscler. Thromb. Vasc. Biol.* **22,** 364–373
8. Jeng, J. Y., Yeh, T. S., Lee, J. W., Lin, S. H., Fong, T. H., and Hsieh, R. H.

(2008) Maintenance of mitochondrial DNA copy number and expression are essential for preservation of mitochondrial function and cell growth. *J. Cell. Biochem.* **103,** 347–357
9. Yi, C. H., Pan, H., Seebacher, J., Jang, I. H., Hyberts, S. G., Heffron, G. J., Vander Heiden, M. G., Yang, R., Li, F., Locasale, J. W., Sharfi, H., Zhai, B., Rodriguez-Mias, R., Luithardt, H., Cantley, L. C., Daley, G. Q., Asara, J. M., Gygi, S. P., Wagner, G., Liu, C. F., and Yuan, J. (2011) Metabolic regulation of protein *N*-α-acetylation by Bcl-x_L promotes cell survival. *Cell* **146,** 607–620
10. Feldenberg, L. R., Thevananther, S., del Rio, M., de Leon, M., and Devarajan, P. (1999) Partial ATP depletion induces Fas- and caspase-mediated apoptosis in MDCK cells. *Am. J. Physiol.* **276,** F837–846
11. Gaspari, M., Larsson, N. G., and Gustafsson, C. M. (2004) The transcription machinery in mammalian mitochondria. *Biochim. Biophys. Acta* **1659,** 148–152
12. Corral-Debrinski, M., Shoffner, J. M., Lott, M. T., and Wallace, D. C. (1992) Association of mitochondrial DNA damage with aging and coronary atherosclerotic heart disease. *Mutat. Res.* **275,** 169–180
13. Larsson, N. G., Wang, J., Wilhelmsson, H., Oldfors, A., Rustin, P., Lewandoski, M., Barsh, G. S., and Clayton, D. A. (1998) Mitochondrial transcription factor A is necessary for mtDNA maintenance and embryogenesis in mice. *Nat. Genet.* **18,** 231–236
14. Ekstrand, M. I., Falkenberg, M., Rantanen, A., Park, C. B., Gaspari, M., Hultenby, K., Rustin, P., Gustafsson, C. M., and Larsson, N. G. (2004) Mitochondrial transcription factor A regulates mtDNA copy number in mammals. *Hum. Mol. Genet* **13,** 935–944
15. Falkenberg, M., Gaspari, M., Rantanen, A., Trifunovic, A., Larsson, N. G., and Gustafsson, C. M. (2002) Mitochondrial transcription factors B1 and B2 activate transcription of human mtDNA. *Nat. Genet.* **31,** 289–294
16. Wang, J., Wilhelmsson, H., Graff, C., Li, H., Oldfors, A., Rustin, P., Brüning, J. C., Kahn, C. R., Clayton, D. A., Barsh, G. S., Thorén, P., and Larsson, N. G. (1999) Dilated cardiomyopathy and atrioventricular conduction blocks induced by heart-specific inactivation of mitochondrial DNA gene expression. *Nat. Genet.* **21,** 133–137
17. Li, H., Wang, J., Wilhelmsson, H., Hansson, A., Thoren, P., Duffy, J., Rustin, P., and Larsson, N. G. (2000) Genetic modification of survival in tissue-specific knockout mice with mitochondrial cardiomyopathy. *Proc. Natl. Acad. Sci. U.S.A.* **97,** 3467–3472
18. Nakamura, T., Imai, Y., Matsumoto, T., Sato, S., Takeuchi, K., Igarashi, K., Harada, Y., Azuma, Y., Krust, A., Yamamoto, Y., Nishina, H., Takeda, S., Takayanagi, H., Metzger, D., Kanno, J., Takaoka, K., Martin, T. J., Chambon, P., and Kato, S. (2007) Estrogen prevents bone loss via estrogen receptor α and induction of Fas ligand in osteoclasts. *Cell* **130,** 811–823
19. Ke, H. Z., Qi, H., Weidema, A. F., Zhang, Q., Panupinthu, N., Crawford, D. T., Grasser, W. A., Paralkar, V. M., Li, M., Audoly, L. P., Gabel, C. A., Jee, W. S., Dixon, S. J., Sims, S. M., and Thompson, D. D. (2003) Deletion of the P2X7 nucleotide receptor reveals its regulatory roles in bone formation and resorption. *Mol. Endocrinol.* **17,** 1356–1367
20. Takahashi, N., Akatsu, T., Udagawa, N., Sasaki, T., Yamaguchi, A., Moseley, J. M., Martin, T. J., and Suda, T. (1988) Osteoblastic cells are involved in osteoclast formation. *Endocrinology* **123,** 2600–2602
21. Miyazaki, T., Katagiri, H., Kanegae, Y., Takayanagi, H., Sawada, Y., Yamamoto, A., Pando, M. P., Asano, T., Verma, I. M., Oda, H., Nakamura, K., and Tanaka, S. (2000) Reciprocal role of ERK and NF-κB pathways in survival and activation of osteoclasts. *J. Cell Biol.* **148,** 333–342
22. Oshima, Y., Akiyama, T., Hikita, A., Iwasawa, M., Nagase, Y., Nakamura, M., Wakeyama, H., Kawamura, N., Ikeda, T., Chung, U. I., Hennighausen, L., Kawaguchi, H., Nakamura, K., and Tanaka, S. (2008) Pivotal role of Bcl-2 family proteins in the regulation of chondrocyte apoptosis. *J. Biol. Chem.* **283,** 26499–26508
23. Akiyama, T., Miyazaki, T., Bouillet, P., Nakamura, K., Strasser, A., and Tanaka, S. (2005) *In vitro* and *in vivo* assays for osteoclast apoptosis. *Biol. Proced. Online* **7,** 48–59
24. Sawada, Y., and Sheetz, M. P. (2002) Force transduction by Triton cytoskeletons. *J. Cell Biol.* **156,** 609–615
25. Sawada, Y., Tamada, M., Dubin-Thaler, B. J., Cherniavskaya, O., Sakai, R., Tanaka, S., and Sheetz, M. P. (2006) Force sensing by mechanical extension of the Src family kinase substrate p130Cas. *Cell* **127,** 1015–1026
26. Orriss, I. R., Knight, G. E., Utting, J. C., Taylor, S. E., Burnstock, G., and Arnett, T. R. (2009) Hypoxia stimulates vesicular ATP release from rat osteoblasts. *J. Cell Physiol.* **220,** 155–162
27. Chen, H., Vermulst, M., Wang, Y. E., Chomyn, A., Prolla, T. A., McCaffery, J. M., and Chan, D. C. (2010) Mitochondrial fusion is required for mtDNA stability in skeletal muscle and tolerance of mtDNA mutations. *Cell* **141,** 280–289
28. Alavian, K. N., Li, H., Collis, L., Bonanni, L., Zeng, L., Sacchetti, S., Lazrove, E., Nabili, P., Flaherty, B., Graham, M., Chen, Y., Messerli, S. M., Mariggio, M. A., Rahner, C., McNay, E., Shore, G. C., Smith, P. J., Hardwick, J. M., and Jonas, E. A. (2011) Bcl-x_L regulates metabolic efficiency of neurons through interaction with the mitochondrial F_1F_O ATP synthase. *Nat. Cell Biol.* **13,** 1224–1233
29. Chen, Y. B., Aon, M. A., Hsu, Y. T., Soane, L., Teng, X., McCaffery, J. M., Cheng, W. C., Qi, B., Li, H., Alavian, K. N., Dayhoff-Brannigan, M., Zou, S., Pineda, F. J., O'Rourke, B., Ko, Y. H., Pedersen, P. L., Kaczmarek, L. K., Jonas, E. A., and Hardwick, J. M. (2011) Bcl-x_L regulates mitochondrial energetics by stabilizing the inner membrane potential. *J. Cell Biol.* **195,** 263–276
30. Miyazaki, T., Neff, L., Tanaka, S., Horne, W. C., and Baron, R. (2003) Regulation of cytochrome *c* oxidase activity by c-Src in osteoclasts. *J. Cell Biol.* **160,** 709–718
31. Nagase, Y., Iwasawa, M., Akiyama, T., Kadono, Y., Nakamura, M., Oshima, Y., Yasui, T., Matsumoto, T., Hirose, J., Nakamura, H., Miyamoto, T., Bouillet, P., Nakamura, K., and Tanaka, S. (2009) Antiapoptotic molecule Bcl-2 regulates the differentiation, activation, and survival of both osteoblasts and osteoclasts. *J. Biol. Chem.* **284,** 36659–36669
32. Takayanagi, H., Kim, S., Koga, T., Nishina, H., Isshiki, M., Yoshida, H., Saiura, A., Isobe, M., Yokochi, T., Inoue, J., Wagner, E. F., Mak, T. W., Kodama, T., and Taniguchi, T. (2002) Induction and activation of the transcription factor NFATc1 (NFAT2) integrate RANKL signaling in terminal differentiation of osteoclasts. *Dev. Cell* **3,** 889–901
33. Winkeler, C. L., Kladney, R. D., Maggi, L. B., Jr., and Weber, J. D. (2012) Cathepsin K-Cre causes unexpected germline deletion of genes in mice. *PLoS One* **7,** e42005
34. Wang, J., Silva, J. P., Gustafsson, C. M., Rustin, P., and Larsson, N. G. (2001) Increased *in vivo* apoptosis in cells lacking mitochondrial DNA gene expression. *Proc. Natl. Acad. Sci. U.S.A.* **98,** 4038–4043
35. Hardie, D. G. (2003) Minireview: The AMP-activated protein kinase cascade: the key sensor of cellular energy status. *Endocrinology* **144,** 5179–5183
36. Schwiebert, E. M., and Zsembery, A. (2003) Extracellular ATP as a signaling molecule for epithelial cells. *Biochim. Biophys. Acta* **1615,** 7–32
37. Chen, Y., Corriden, R., Inoue, Y., Yip, L., Hashiguchi, N., Zinkernagel, A., Nizet, V., Insel, P. A., and Junger, W. G. (2006) ATP release guides neutrophil chemotaxis via $P2Y_2$ and A3 receptors. *Science* **314,** 1792–1795
38. Morelli, A., Chiozzi, P., Chiesa, A., Ferrari, D., Sanz, J. M., Falzoni, S., Pinton, P., Rizzuto, R., Olson, M. F., and Di Virgilio, F. (2003) Extracellular ATP causes ROCK I-dependent bleb formation in P2X7-transfected HEK293 cells. *Mol. Biol. Cell* **14,** 2655–2664
39. Hwang, S. M., Li, J., Koo, N. Y., Choi, S. Y., Lee, S. J., Oh, S. B., Castro, R., Kim, J. S., and Park, K. (2009) Role of purinergic receptor in α-fodrin degradation in Par C5 cells. *J. Dent. Res.* **88,** 927–932
40. Martin, S. J., O'Brien, G. A., Nishioka, W. K., McGahon, A. J., Mahboubi, A., Saido, T. C., and Green, D. R. (1995) Proteolysis of fodrin (non-erythroid spectrin) during apoptosis. *J. Biol. Chem.* **270,** 6425–6428
41. Auger, R., Motta, I., Benihoud, K., Ojcius, D. M., and Kanellopoulos, J. M. (2005) A role for mitogen-activated protein kinase(Erk1/2) activation and non-selective pore formation in P2X7 receptor-mediated thymocyte death. *J. Biol. Chem.* **280,** 28142–28151
42. Iglesias, R., Locovei, S., Roque, A., Alberto, A. P., Dahl, G., Spray, D. C., and Scemes, E. (2008) P2X7 receptor-Pannexin 1 complex: pharmacology and signaling. *Am. J. Physiol. Cell Physiol.* **295,** C752–C760
43. Pellegatti, P., Falzoni, S., Donvito, G., Lemaire, I., and Di Virgilio, F. (2011) P2X7 receptor drives osteoclast fusion by increasing the extracellular adenosine concentration. *FASEB J.* **25,** 1264–1274
44. Wallace, D. C. (1992) Mitochondrial genetics: a paradigm for aging and degenerative diseases? *Science* **256,** 628–632

45. Barazzoni, R., Short, K. R., and Nair, K. S. (2000) Effects of aging on mitochondrial DNA copy number and cytochrome *c* oxidase gene expression in rat skeletal muscle, liver, and heart. *J. Biol. Chem.* **275,** 3343–3347
46. Halloran, B. P., Ferguson, V. L., Simske, S. J., Burghardt, A., Venton, L. L., and Majumdar, S. (2002) Changes in bone structure and mass with advancing age in the male C57BL/6J mouse. *J. Bone Miner Res.* **17,** 1044–1050
47. Matsumoto, T., Nagase, Y., Iwasawa, M., Yasui, T., Masuda, H., Kadono, Y., Nakamura, K., and Tanaka, S. (2011) Distinguishing the proapoptotic and antiresorptive functions of risedronate in murine osteoclasts: role of the Akt pathway and the ERK/Bim axis. *Arthritis Rheum.* **63,** 3908–3917
48. Izyumov, D. S., Avetisyan, A. V., Pletjushkina, O. Y., Sakharov, D. V., Wirtz, K. W., Chernyak, B. V., and Skulachev, V. P. (2004) "Wages of fear": transient threefold decrease in intracellular ATP level imposes apoptosis. *Biochim. Biophys. Acta* **1658,** 141–147
49. Duong, L. T., Lakkakorpi, P., Nakamura, I., and Rodan, G. A. (2000) Integrins and signaling in osteoclast function. *Matrix Biol.* **19,** 97–105
50. Gil-Henn, H., Destaing, O., Sims, N. A., Aoki, K., Alles, N., Neff, L., Sanjay, A., Bruzzaniti, A., De Camilli, P., Baron, R., and Schlessinger, J. (2007) Defective microtubule-dependent podosome organization in osteoclasts leads to increased bone density in *Pyk2*$^{-/-}$ mice. *J. Cell Biol.* **178,** 1053–1064
51. Miller, D. S., and Horowitz, S. B. (1986) Intracellular compartmentalization of adenosine triphosphate. *J. Biol. Chem.* **261,** 13911–13915
52. Fields, R. D. (2011) Nonsynaptic and nonvesicular ATP release from neurons and relevance to neuron-glia signaling. *Semin. Cell Dev. Biol.* **22,** 214–219
53. Praetorius, H. A., and Leipziger, J. (2009) ATP release from non-excitable cells. *Purinergic Signal.* **5,** 433–446
54. Huang, Y., Grinspan, J. B., Abrams, C. K., and Scherer, S. S. (2007) Pannexin 1 is expressed by neurons and glia but does not form functional gap junctions. *Glia* **55,** 46–56
55. Boassa, D., Ambrosi, C., Qiu, F., Dahl, G., Gaietta, G., and Sosinsky, G. (2007) Pannexin 1 channels contain a glycosylation site that targets the hexamer to the plasma membrane. *J. Biol. Chem.* **282,** 31733–31743
56. MacVicar, B. A., and Thompson, R. J. (2010) Non-junction functions of pannexin 1 channels. *Trends Neurosci.* **33,** 93–102
57. Hazama, R., Qu, X., Yokoyama, K., Tanaka, C., Kinoshita, E., He, J., Takahashi, S., Tohyama, K., Yamamura, H., and Tohyama, Y. (2009) ATP-induced osteoclast function: the formation of sealing-zone like structure and the secretion of lytic granules via microtubule-deacetylation under the control of Syk. *Genes Cells* **14,** 871–884
58. Pederson, L., Ruan, M., Westendorf, J. J., Khosla, S., and Oursler, M. J. (2008) Regulation of bone formation by osteoclasts involves Wnt/BMP signaling and the chemokine sphingosine-1-phosphate. *Proc. Natl. Acad. Sci. U.S.A.* **105,** 20764–20769
59. Panupinthu, N., Rogers, J. T., Zhao, L., Solano-Flores, L. P., Possmayer, F., Sims, S. M., and Dixon, S. J. (2008) P2X7 receptors on osteoblasts couple to production of lysophosphatidic acid: a signaling axis promoting osteogenesis. *J. Cell Biol.* **181,** 859–871
60. Genetos, D. C., Geist, D. J., Liu, D., Donahue, H. J., and Duncan, R. L. (2005) Fluid shear-induced ATP secretion mediates prostaglandin release in MC3T3-E1 osteoblasts. *J. Bone Miner. Res.* **20,** 41–49
61. Katz, S., Ayala, V., Santillán, G., and Boland, R. (2011) Activation of the PI3K/Akt signaling pathway through $P2Y_2$ receptors by extracellular ATP is involved in osteoblastic cell proliferation. *Arch. Biochem. Biophys.* **513,** 144–152
62. Li, J., Liu, D., Ke, H. Z., Duncan, R. L., and Turner, C. H. (2005) The P2X7 nucleotide receptor mediates skeletal mechanotransduction. *J. Biol. Chem.* **280,** 42952–42959
63. Wishart, J. M., Need, A. G., Horowitz, M., Morris, H. A., and Nordin, B. E. (1995) Effect of age on bone density and bone turnover in men. *Clin. Endocrinol. (Oxf.)* **42,** 141–146
64. Fatayerji, D., and Eastell, R. (1999) Age-related changes in bone turnover in men. *J. Bone Miner. Res.* **14,** 1203–1210
65. Gallagher, J. C., Kinyamu, H. K., Fowler, S. E., Dawson-Hughes, B., Dalsky, G. P., and Sherman, S. S. (1998) Calciotropic hormones and bone markers in the elderly. *J. Bone Miner. Res.* **13,** 475–482
66. Clarke, B. L., Ebeling, P. R., Jones, J. D., Wahner, H. W., O'Fallon, W. M., Riggs, B. L., and Fitzpatrick, L. A. (2002) Predictors of bone mineral density in aging healthy men varies by skeletal site. *Calcif. Tissue Int.* **70,** 137–145